NASA/TM—2017–219431

Hypersonic Inflatable Aerodynamic Decelerator (HIAD) Torus Mechanical Testing

Tony Chen, Matthew R. Moholt, and Larry D.Hudson
Armstrong Flight Research Center, Edwards, California

November 2017

NASA STI Program ... in Profile

Since its founding, NASA has been dedicated to the advancement of aeronautics and space science. The NASA scientific and technical information (STI) program plays a key part in helping NASA maintain this important role.

The NASA STI program operates under the auspices of the Agency Chief Information Officer. It collects, organizes, provides for archiving, and disseminates NASA's STI. The NASA STI program provides access to the NTRS Registered and its public interface, the NASA Technical Reports Server, thus providing one of the largest collections of aeronautical and space science STI in the world. Results are published in both non-NASA channels and by NASA in the NASA STI Report Series, which includes the following report types:

- TECHNICAL PUBLICATION. Reports of completed research or a major significant phase of research that present the results of NASA Programs and include extensive data or theoretical analysis. Includes compilations of significant scientific and technical data and information deemed to be of continuing reference value. NASA counterpart of peer-reviewed formal professional papers but has less stringent limitations on manuscript length and extent of graphic presentations.

- TECHNICAL MEMORANDUM. Scientific and technical findings that are preliminary or of specialized interest, e.g., quick release reports, working papers, and bibliographies that contain minimal annotation. Does not contain extensive analysis.

- CONTRACTOR REPORT. Scientific and technical findings by NASA-sponsored contractors and grantees.

- CONFERENCE PUBLICATION. Collected papers from scientific and technical conferences, symposia, seminars, or other meetings sponsored or co-sponsored by NASA.

- SPECIAL PUBLICATION. Scientific, technical, or historical information from NASA programs, projects, and missions, often concerned with subjects having substantial public interest.

- TECHNICAL TRANSLATION. English-language translations of foreign scientific and technical material pertinent to NASA's mission.

Specialized services also include organizing and publishing research results, distributing specialized research announcements and feeds, providing information desk and personal search support, and enabling data exchange services.

For more information about the NASA STI program, see the following:

- Access the NASA STI program home page at http://www.sti.nasa.gov

- E-mail your question to help@sti.nasa.gov

- Phone the NASA STI Information Desk at 757-864-9658

- Write to:
  NASA STI Information Desk
  Mail Stop 148
  NASA Langley Research Center
  Hampton, VA 23681-2199

NASA/TM—2017–219431

Hypersonic Inflatable Aerodynamic Decelerator (HIAD) Torus Mechanical Testing

Tony Chen, Matthew R. Moholt, and Larry D.Hudson
Armstrong Flight Research Center, Edwards, California

National Aeronautics and
Space Administration

Armstrong Flight Research Center
Edwards, California 93523-0273

November 2017

Table of Contents

Figures

Tables

Abstract

The National Aeronautics and Space Administration (NASA) Armstrong Flight Research Center (Edwards, California) has performed loads testing of a series of developmental atmospheric entry decelerator structural components. Test setup hardware were designed and fabricated. In addition, a test plan and checklist were developed to enable the consistent and efficient execution of the tests. Eight test articles were successfully tested in over 100 test runs. Test article buckling shapes and buckling loads were observed. Displacements and strains were recorded as various load cases were applied. The test data were sent to the NASA Langley Research Center (Hampton, Virginia) to help with the validation and construction of the finite element model of the HIAD assembly.

Nomenclature

AFRC	Armstrong Flight Research Center
DAS	data acquisition system
FEM	finite element model
FLL	Flight Loads Laboratory
HIAD	Hypersonic Inflatable Aerodynamic Decelerator
IADS®	Interactive Analysis and Display System
LaRC	Langley Research Center
LC	load cell
LCB	load cell bottom
LCT	load cell top
LMSG	liquid metal strain gage
LRT	linear resistance transducer
LT	load train
MLCS	mechanical load control system
POT, pot	potentiometer
SG	strain gage

1.0 Introduction

In order to achieve greater payload capacities for future exploration missions, a new method of atmospheric entry must be developed. A new entry, descent, and landing (EDL) architecture is being developed that utilizes an advanced deployable decelerator, allowing heavier payloads by lowering the ballistic coefficient. One of the space technologies being investigated by the National Aeronautics and Space Administration (NASA) Game Changing Development Program (GCD) of the NASA Space Technology Mission Directorate (STMD) is the Hypersonic Inflatable Aerodynamic Decelerator (HIAD). The new hypersonic decelerator design, which is comprised of a series of tori of diminishing sizes, could enable NASA to land heavy payloads safely on the surfaces of other planets. The deflated structure would be stowed for launch, and deployed in its conical aeroshell shape prior to atmospheric entry (entry depicted in figure 1). The HIAD Project is being managed and developed by the NASA Langley Research Center (LaRC) (Hampton, Virginia), who also defined the test requirements and developed the initial test matrix.

Figure 1. Depiction of the HIAD entering Earth's atmosphere.

In order to validate the finite element models (FEMs) used in the structural analyses of the HIAD, laboratory testing of the HIAD torus elements was required. The Flight Loads Laboratory (FLL) (figure 2) at the NASA Armstrong Flight Research Center (AFRC) was chosen to design and perform the HIAD elemental, mechanical loads testing. This testing was performed on individual tori of the 20-ft (6-m) diameter HIAD structure design.

Figure 2. The NASA Armstrong Flight Research Center Flight Loads Laboratory.

This report summarizes the completed HIAD torus mechanical testing that was performed in the FLL. The test objectives, test setup hardware, instrumentation, test operation, observations, and brief summary of data are discussed.

2.0 Test Objectives

The purpose of the mechanical loads tests was to characterize the structural properties of the torus-shaped test articles. The two types of testing were compression and torsion. One of the test objectives was to demonstrate and determine the onset of buckling; the other objective was to obtain constitutive data from instrumentation to help in constructing the FEM.

Test success criteria were defined as follows:

- Test article buckling was achieved through the application of load as specified in appendix A, and
- Required data were obtained (list shown in section 6.11).

3.0 Test Article Description

All test articles were torus-shaped and had a tube diameter of 13.6 in. Geometrically, there were three different sizes, denoted as T3, T4, and T5, with outside diameters of 11 ft, 13 ft, and 15 ft, respectively. The HIAD test articles were constructed with Technora® (Teijin Limited, Osaka, Japan) braided fabric and a layer of urethane as the gas barrier. Two axial cords constructed of the same fabric material were embedded near the inner radius to provide structural rigidity. There were four ports for inflation and deflation, spaced 90 deg apart, as shown in figure 3.

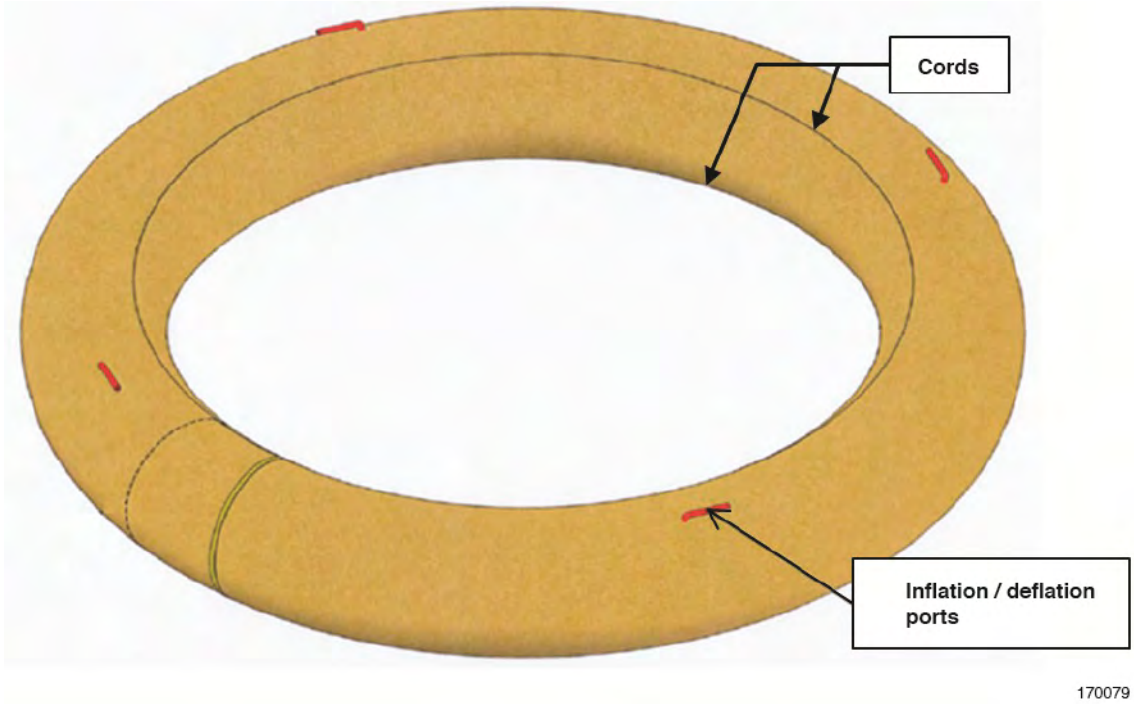

Figure 3. Torus-shaped HIAD test article showing structural rigidity cords and the four inflation and deflation ports.

In addition to the different diameters, the test articles also varied by cord types and braid angles. There were a total of eight unique test articles (table 1) except for T4A-1 and T4A-2, which were identical and tested in order to examine repeatability. Each test article was pressure-tested by the manufacturer prior to shipping to NASA.

Table 1. List of test articles.

Test Article No.	Test Article Serial No.	Tube Diameter	Outer Diameter	Cord Strength	Braid Angle	Max Test Pressure	Max Operating Pressure	Acceptance Test Pressure
		(in)	(ft)		(deg)	(psi)	(psi)	(psi)
1	T3A-1	13	11	strong	71	20	25	30
2	T4A-1	13	13	strong	71	20	25	30
3	T4A-2	13	13	strong	71	20	25	30
4	T4A-3	13	13	weak	71	15	20	25
5	T5A-1	13	15	strong	71	20	25	30
6	T5B-1	13	15	weak	64	20	25	30
7	T5B-2	13	15	strong	64	20	25	30
8	T5C-1	13	15	strong	60	20	25	30

So that loads could be applied to the test article, 32 straps were circumferentially bonded, equally spaced, to each test article (figure 4). Buffer straps (figure 5), used to help evenly distribute applied loads, were first bonded to the test article, and the loading straps were bonded onto them. This work was done prior to shipment of the test article to the FLL. At the end of each of the straps is a D-ring used for attaching the loading hardware.

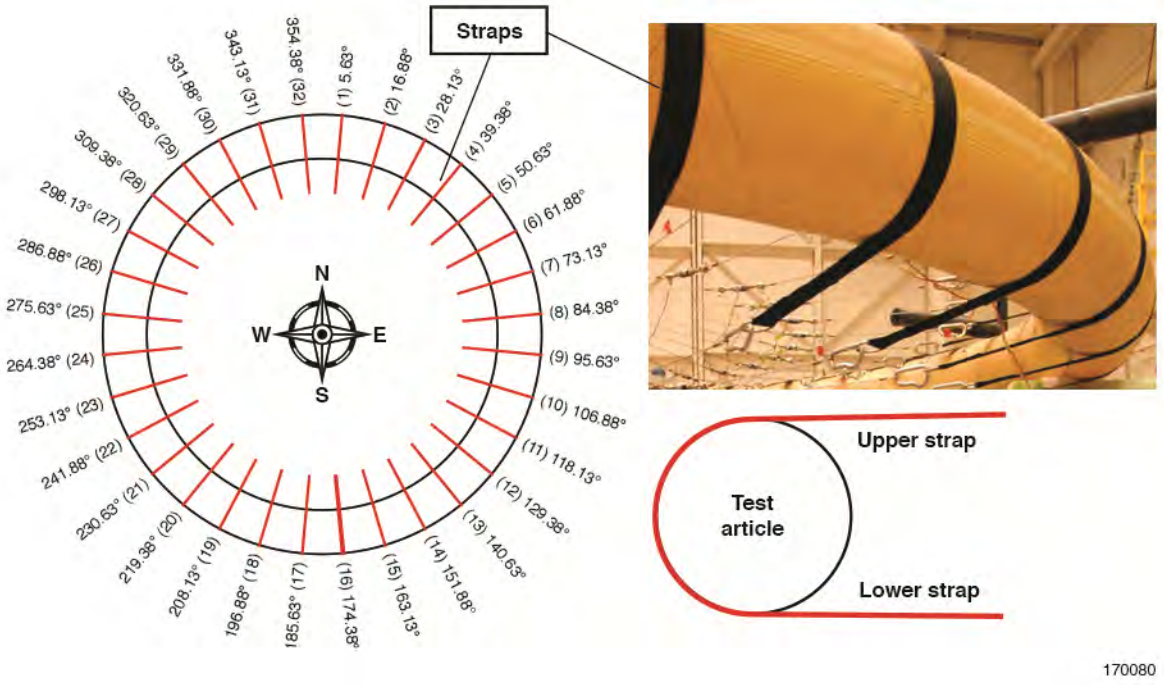

Figure 4. Straps bonded to the HIAD test article for load train attachment.

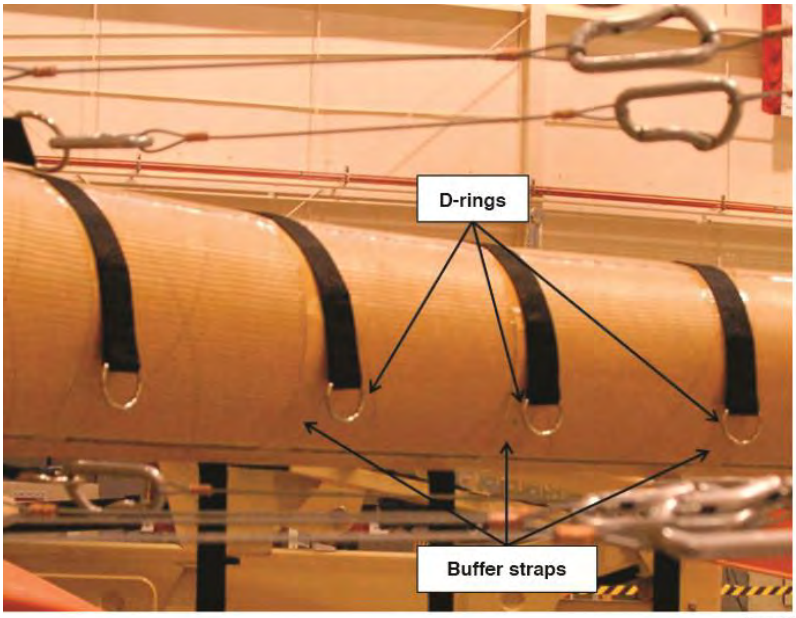

Figure 5. The HIAD test article, showing the buffer straps and the D-ring attached to the end of each strap.

4.0 Test Description

There were two types of load cases: Compression and torsion. In the compression load cases, equal loads were applied to each strap-end at the D-ring, pulling it toward the center of the test article. In the torsion load cases, loads applied at the upper strap-ends were higher than loads applied at the bottom strap-ends, to create torsional loads. Figure 6 illustrates the manner in which the loadings were applied in each type of load case.

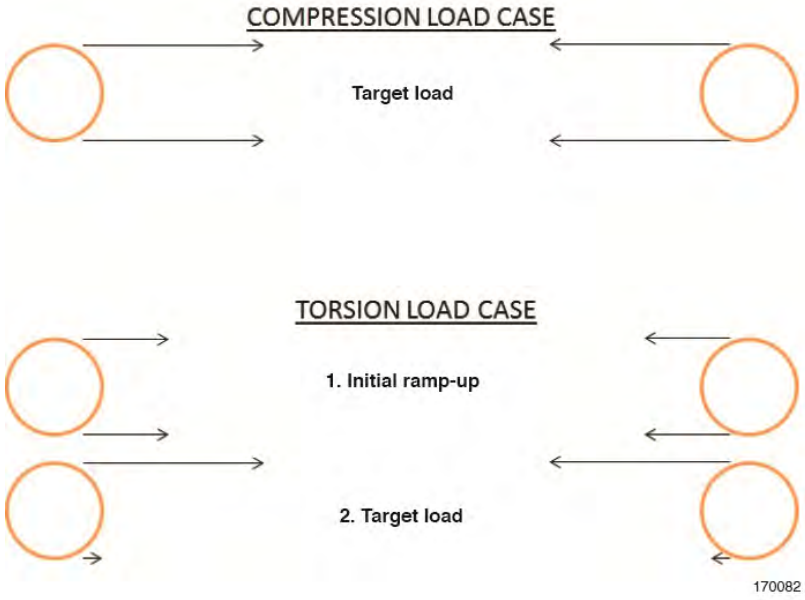

Figure 6. Load case diagrams illustrating the application of the two types of external loads.

For both types of load cases, the loads were applied until either the target load was reached or until buckling (structural instability) occurred. The applied loads, the test article cord strains, and the test article displacements were measured and recorded. Representative load profiles for the compression load cases and the torsion load cases are illustrated in figure 7 and figure 8, respectively.

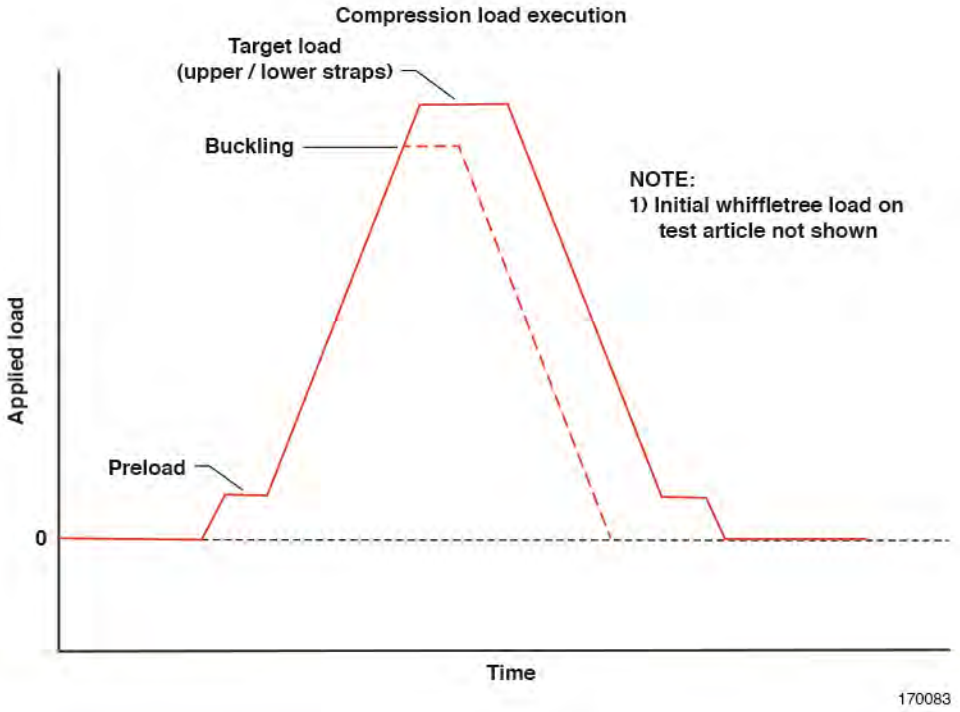

Figure 7. Representative load profile for the compression load cases.

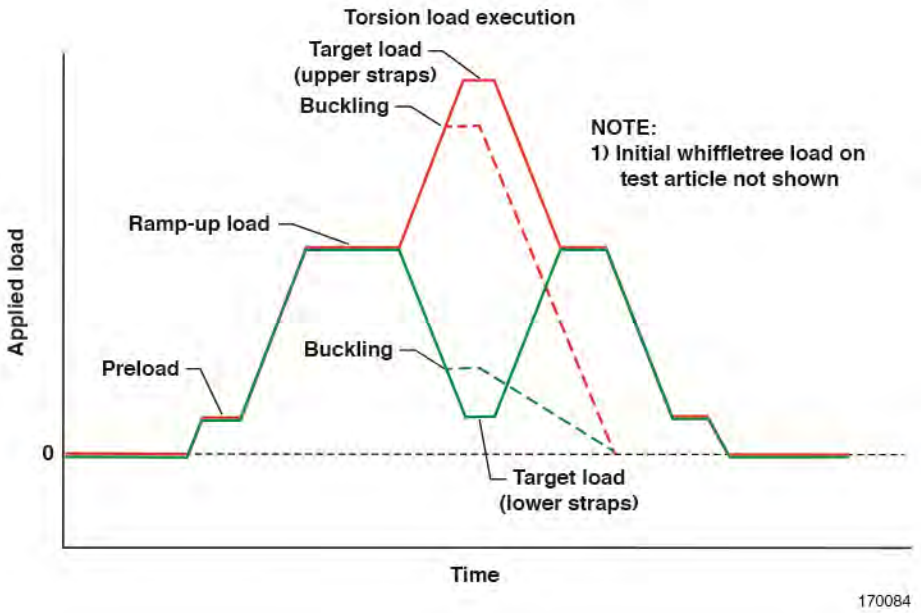

Figure 8. Representative load profile for the torsion load cases.

The test matrix in the test plan specified both compression and torsion tests to be executed at pressures of 20, 15, 10, and 5 psi. The only exception was for test article T4A-3, which had a maximum test pressure of 15 psi due to its lower cord strength. The test matrix is listed in appendix A. The initial compression and torsion test cases for each test article were planned to be repeated three times, while all subsequent test cases were planned to be repeated twice. During testing, however, due to unexpected test results and time constraint, decisions were made, with NASA LaRC concurrence, to repeat or skip some of the tests to best achieve test objectives. The tests conducted are shown in tables in section 8.2, "Test Summary."

After the completion of testing of the first two test articles, NASA LaRC requested that pre-test and post-test measurements of the test articles be performed to calculate the braid angles (figure 9).

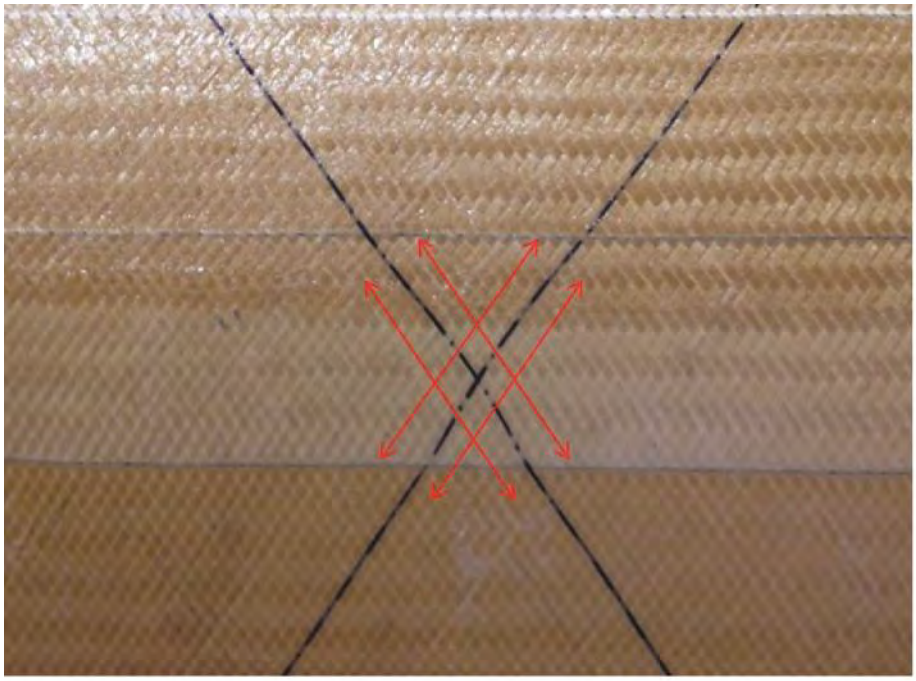

Figure 9. Braid fabric directions.

The braid angles were calculated by inflating the test article to 15 psi and then measuring the distance between each tracer thread crossing along the outer radius and inner radius. The circumference of the torus tube was also measured at each tracer thread crossing (figure 10). In addition, photogrammetry data were taken from above the test article in order to obtain the target locations placed on the tracer thread crossings on the top of the test article. The pre-test data provided information on any crossing-to-crossing variations in the as-fabricated test article. The pre-test and post-test measurement comparison was used to help evaluating the condition of the test article after testing. Appendix B presents the results of these measurements.

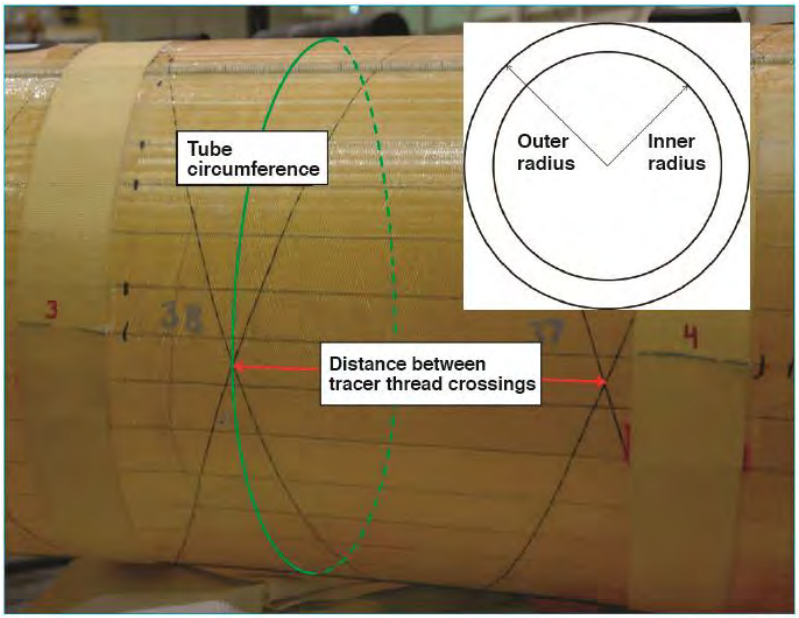

Figure 10. Pre-test and post-test tracer thread crossing and circumference measurements.

5.0 Test Setup

The layout of the test equipment and test personnel are shown in figure 11. Most of the test personnel were stationed in the test area around the test article. The Load Control Operator and the Video/Communication Operator, however, were stationed in the FLL control room due to the location of their assigned systems. The Test Conductor and the Load Control Operator needed to maintain uninterrupted communication during testing, so the Test Conductor was also stationed in the FLL control room.

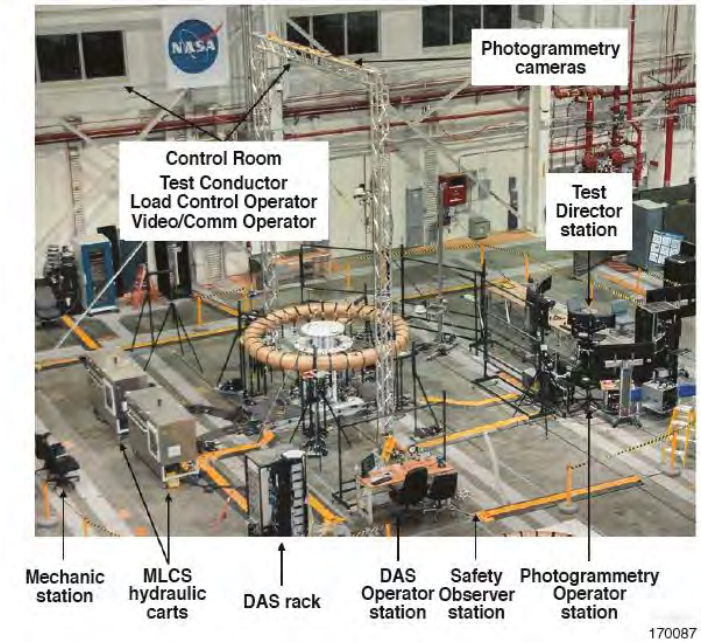

Figure 11. The test area in the Flight Loads Laboratory, showing assigned stations for test personnel.

5.1 Test Setup Hardware

This section discusses the design approach of the test setup hardware. An overview of the primary equipment is also presented.

5.1.1 Design Approach

Test setup design and solid modeling were performed in PTC Creo® (Parametric Technology Corporation, Needham, Massachusetts) computer-aided design software. A requisite of the test was that the torus be supported in such a fashion that it was free to rotate and deflect so as not to influence the onset of buckling. The compression and torsion loads were to be introduced to the test article evenly and consistently during test article deflection to prevent premature buckling caused by localized loading.

A simple-design philosophy was carried throughout the design cycle and sought to reduce cost by ensuring the ease of manufacture and assembly of all hardware. Technicians and fabricators were involved early in the development of the design. The realization of the simple-design approach can be seen in the 100-plus, 1-in thick steel plate pulley mount holes in the hub stand and in the ring stand. By designing the steel plates to fit on the AFRC water-jet machine for drilling the pulley mount holes, a significant amount of time was saved as opposed to the time that would be necessary to drill the holes using traditional methods.

5.1.2 Preliminary Concepts

The objective of the test program was to buckle each torus under a known compression or torsion load. The original concept was to introduce load to the outer perimeter as evenly as possible using a pressurized air bag. This approach, depicted in figure 12, employed a pressurized air bag that applied pressure to hard foam pads that were evenly spaced around the torus. The significant number of pads would each require machining to mate to the surface of the torus. Each torus size would require its own set of foam pads and test apparatus. Additional challenges to the execution of this approach were that each foam pad would have to be carefully set in place, and the pressurized air bag would need to inflate with very precise alignment. While this method was considered for a compression test approach, the design could not enable introducing torsion loads, which would require a completely different test setup. Understandably, this design was rejected in favor of a more feasible approach.

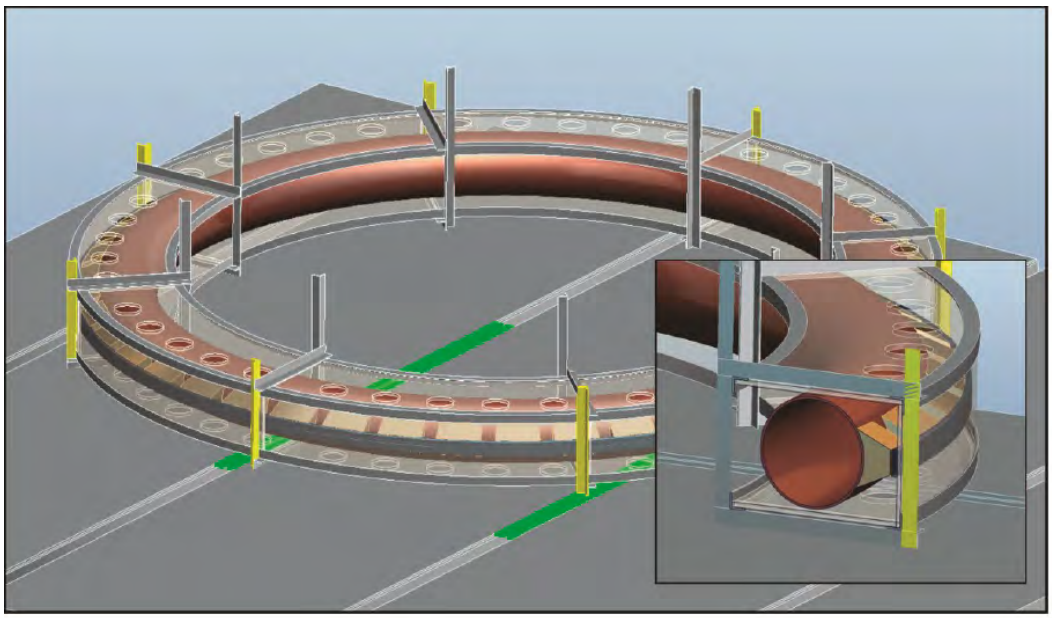

Figure 12. The original compression test concept utilizing a pressurized air bag.

The second approach utilized straps which would be evenly bonded to the outside tube portion of the torus. An analysis was performed and it was determined that 32 straps would sufficiently introduce the loads uniformly without causing localized "point load" effects. A challenge of this approach was that each strap-end would need to be controlled independently to ensure even loading during asymmetric torus deflection. For this reason it was originally envisioned to place hydraulic jacks near the center of the torus to load each strap-end, which would require a total of 64 jacks. Figure 13 shows this arrangement for eight straps and demonstrates the lack of feasibility for 32 jacks. Furthermore, the FLL simply did not have enough hydraulic jacks for this approach.

A variation to the second approach, which was ultimately the chosen design, utilized a whiffletree system that allowed one jack to control four strap-ends. A whiffletree system consists of a number of pivoted bars that divide a single applied load on the center crossbar into smaller load components. The whiffletree system approach was enabled by elevating the test article and connecting the strap-ends to steel cables, which were then directed down by way of pulleys to the whiffletree system. This method also allowed the upper strap-ends to be controlled independently from the lower strap-ends, thus allowing a torsion load to be introduced by placing more load on the upper or lower straps.

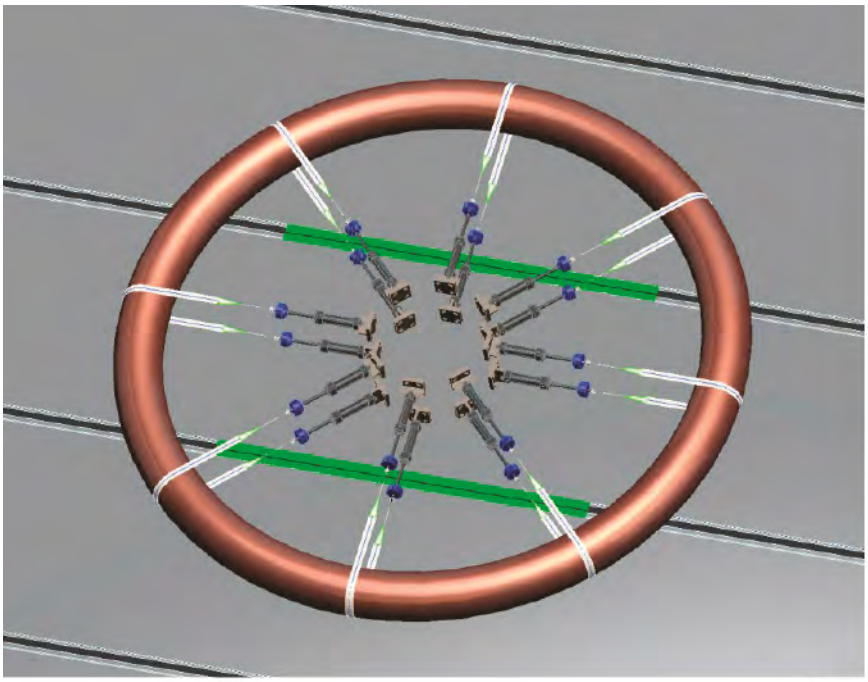

170089

Figure 13. The second design concept, utilizing hydraulic jacks.

5.1.3 Flight Loads Laboratory Design Requirements

To ensure safety, all test fixture hardware in the FLL is required to meet a design factor of safety of 2.0 based upon yield strength or 3.0 based on ultimate strength. Therefore, all hardware for the test program was designed to satisfy this design requirement. The load cables, although sized to meet the safety factor requirements, still required proof loading to two times the maximum load to verify the quality of the crimped loop ends.

5.1.4 Primary Equipment

The test setup (figure 14) consisted of four primary sub-assemblies, which are detailed in this section. The sub-assemblies included the load train, hub stand, ring stand, and test stands.

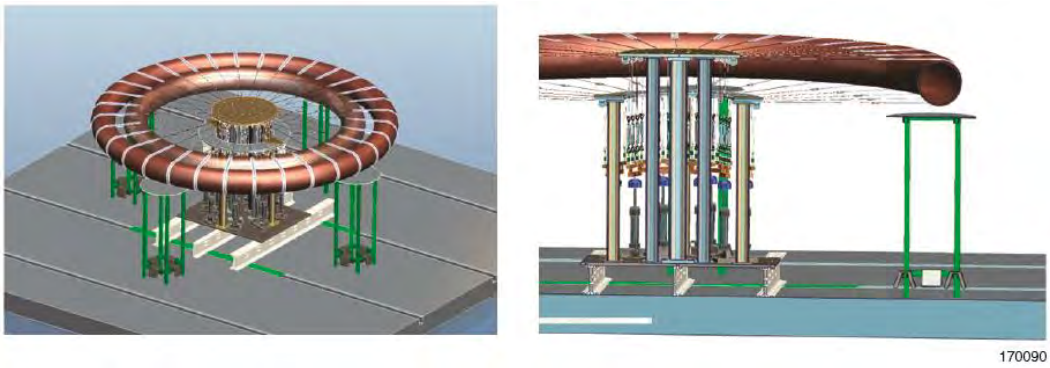

Figure 14. A solid model of the entire T5 test setup; note the smaller T3 torus displayed for size comparison.

5.1.4.1 Load Train - As previously mentioned, each strap-end ultimately terminated at a whiffletree, and each whiffletree was connected to four straps. Figure 15 shows the load train from the jack base to the turnbuckles. Strap length adjustments were made with 4-in turnbuckles and were used to level the whiffletrees prior to loading. Load was controlled and monitored using low-profile 2,000-lbf-capacity load cells that were mounted between the whiffletree and the hydraulic jack. Load was applied using 1.5-in bore hydraulic jacks.

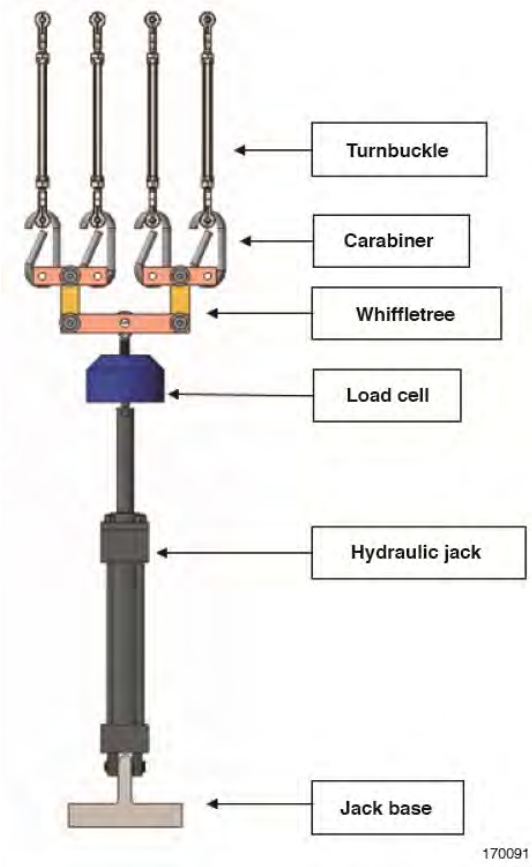

Figure 15. Load train model from hydraulic jack to turnbuckles.

5.1.4.2 Hub Stand - The hub stand (resembling a bicycle hub when fully assembled and shown in Figure 16) provided a platform to support the upper cable pulleys. As previously mentioned, a 1-in thick steel plate provided a mounting surface for the 32 top strap pulleys, supported by four columns made from 4-in schedule 80 steel pipe. Each column was bolted to a 1-in thick steel baseplate that had been water-jet cut to include all the necessary assembly through-holes. The FLL steel C-channel erector set provided the means to bolt the assembly to the floor and did so by acting as the interface between the baseplate and the FLL floor tracks, thus the additional benefit of raising the baseplate to allow hydraulic and instrumentation lines to be routed underneath. The vertical portion of the load train was located under the pulleys.

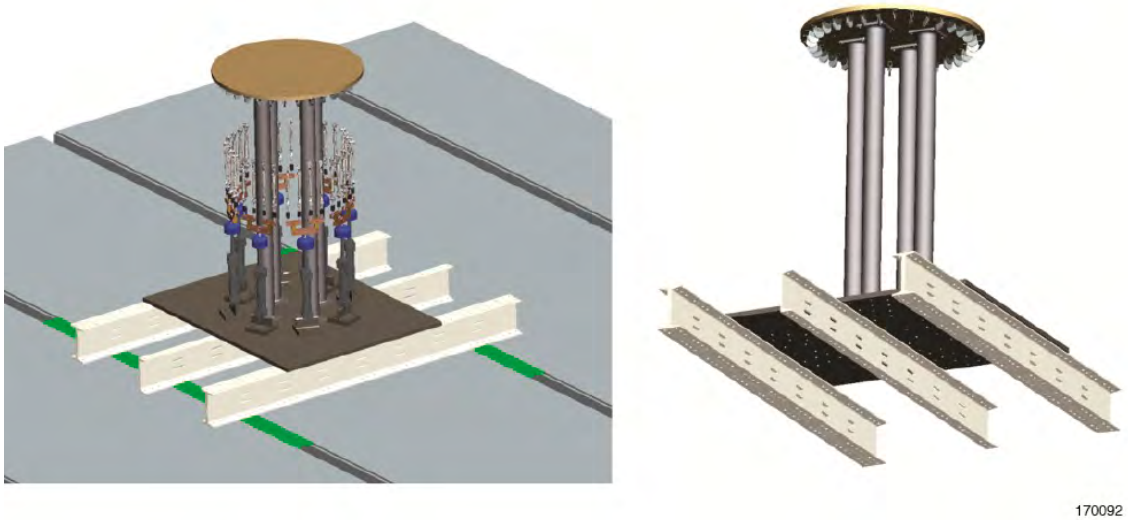

Figure 16. The hub stand installed on the Flight Loads Laboratory erector set.

5.1.4.3 Ring Stand - To support the lower pulleys, a ring stand (figure 17) was designed which would fit around the hub stand. Like the hub stand, it was made of 1-in thick steel plate supported by four 4-in schedule 80 steel columns. Due to its larger size, the ring plate was made as two pieces in order to fit on the water-jet table. The two halves were bolted together as a butt joint and used a top doubler plate for reinforcement. Also, like the hub stand, there were eight whiffletree systems to pull on the 32 lower cables.

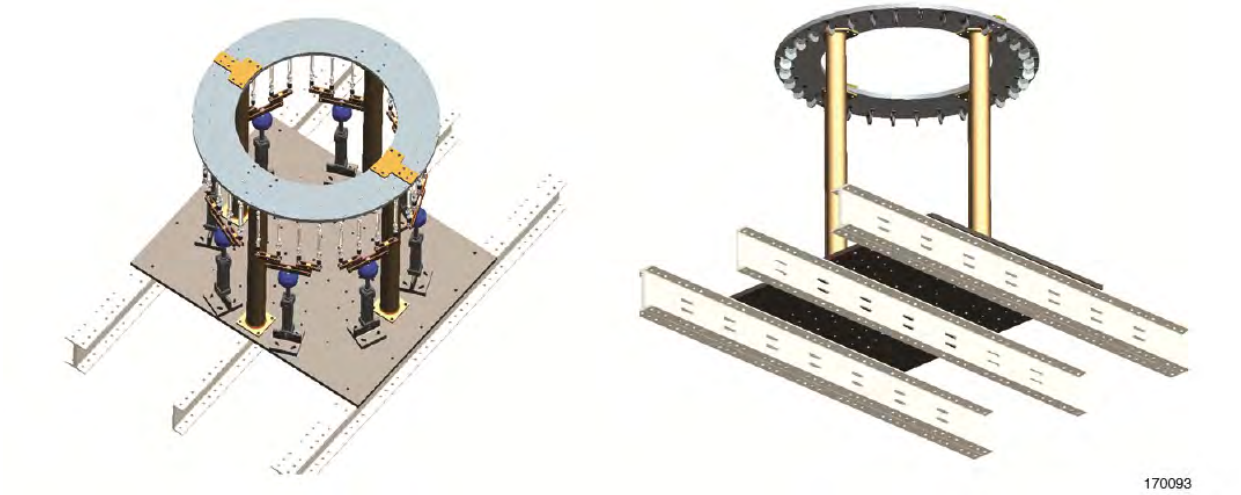

Figure 17. The ring stand installed on the Flight Loads Laboratory erector set.

The hub stand was the first element to be assembled on the steel baseplate. As seen in figure 18, the ring stand was subsequently assembled around it. The configuration was thus fairly tight, but manageable.

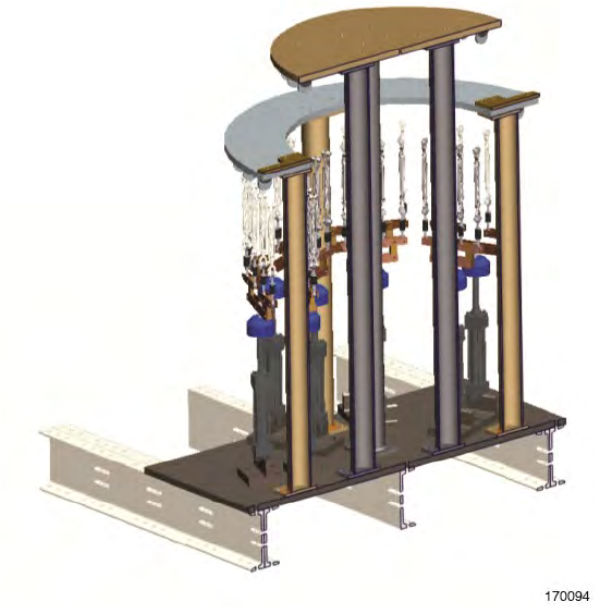

Figure 18. Cross-section view of the hub stand and the ring stand.

5.4.1.4 Test Stands - To support the elevated test article, a set of four test stands was constructed from strut channels. The stands, shown in figure 19, were built intentionally short so the test article could be shimmed with foam to be levelled with the pulleys so that loads could be applied horizontally to prevent out-of-plane loading. A plastic film and cloth were place between the test article and foam to minimize friction at the interface.

Figure 19. A test stand supporting the test article.

5.1.4.5 Test Article Arrestors - To limit the amount of deflection during buckling, a set of six test article arrestors (figure 20) were built and placed around each torus. Restraining the out-of-plane buckling deflection would help prevent damage both to the test article and the test setup hardware. Each stop was set approximately 4 in above the test article.

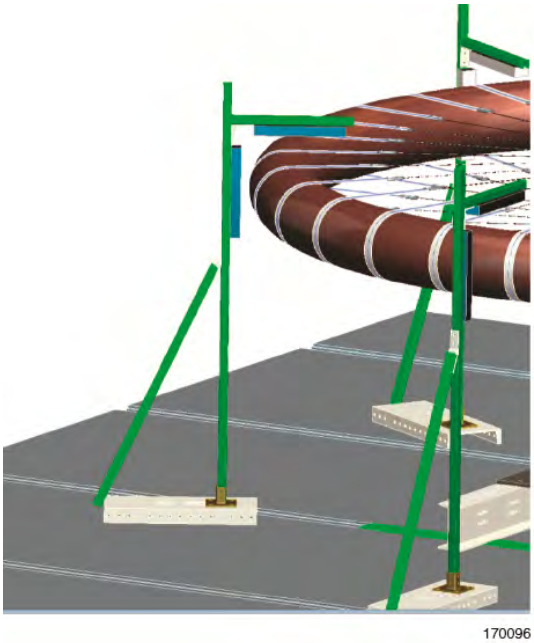

Figure 20. Test article arrestors.

5.1.5 Design Reviews

Preliminary and Critical Design Reviews were held during the hardware development process to allow all testing participants to evaluate and provide feedback on the design details. In addition, the reviews ensured that the test setup design would meet the test requirements.

5.2 Pneumatic System

A pneumatic system (figure 21) was used to inflate and deflate the test article. The pneumatic system regulated the flow rate and pressure of the shop air that was used in the inflation and deflation process. This system was disconnected from the test article and inflation port was closed during loading to prevent airflow.

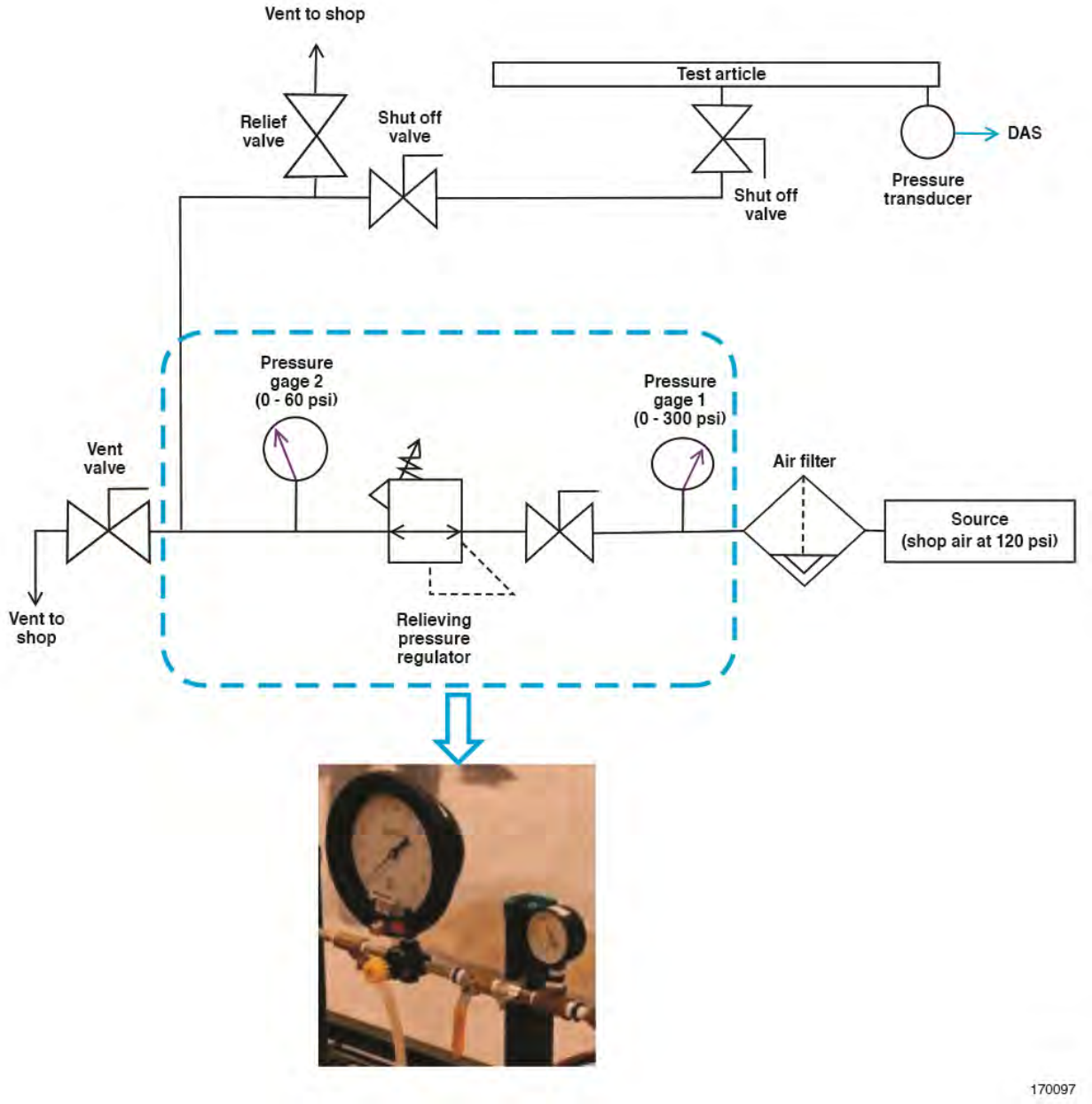

Figure 21. The pneumatic system that was used to inflate and deflate the test article.

5.3 Communication System

All on-site test personnel were equipped with wireless headsets. This communication system was also accessible to off-site test personnel at NASA LaRC by way of the NASA teleconference system.

5.4 Mechanical Load Control System

The FLL 80-channel mechanical load control system (MLCS) was used to support mechanical loading of the test articles. Two hydraulic carts (figure 22) with eight channels per cart were used to control 16 load control channels. Control was performed with force feedback from the load cells. Given the rather unconstrained nature of the test it was originally expected that stroke control would be required because the

test article could deform abruptly. Stroke control was not necessary, however, because the MLCS was able to control each jack using force control with minimum load error throughout the load profile.

Figure 22. The hydraulic carts used for hydraulic actuator control.

6.0 Instrument and Data Collection

In order to monitor test condition and to capture test article responses, several types of instrumentation were put in place to collect data. The test data not only provided information for FEM validation, but the real-time data monitoring was critical to ensure the success and safety of the test execution. The following sections describe the instrumentation; detailed information such as channel name, range of transducer, and measurement locations are presented in appendix C.

6.1 String Displacement Potentiometer

Eight horizontal and eight vertical string displacement potentiometers (pots) were used to measure the test article radial and vertical displacements. Displacements measurements were made every 45 deg, as shown in figure 23.

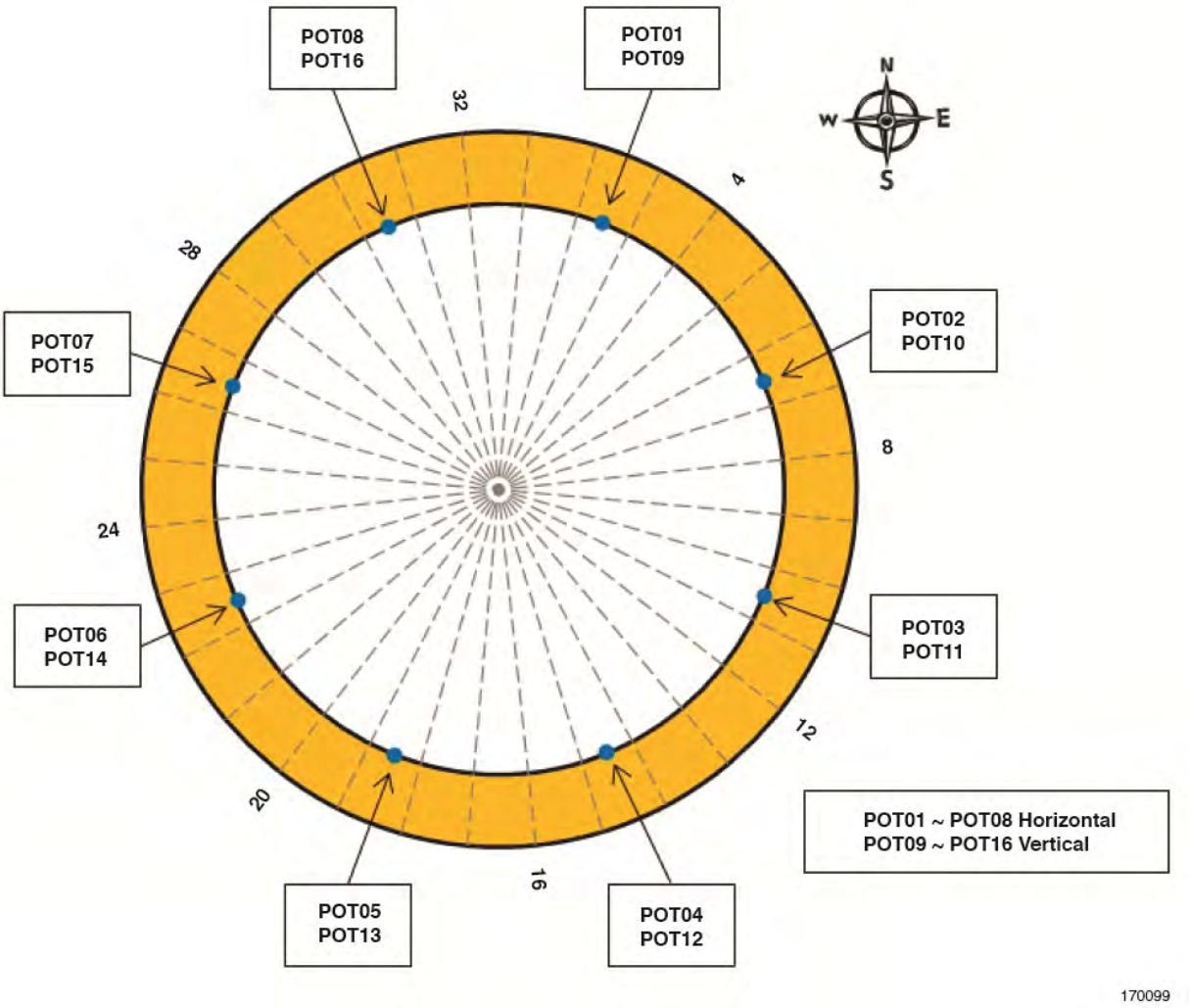

Figure 23. String displacement potentiometer attachment locations.

The string displacement potentiometers for the horizontal displacement measurements were located on the upper surface of the ring stand with the string extending radially outward to the inner radius of the torus (see figure 24). The string displacement potentiometers for the vertical displacement measurements were placed on the floor with the string extending upward to the same inner radius attachment points as the horizontal string pots. The ends of the potentiometer steel wire were attached to metallic tabs which were bonded to the test article by using silicone adhesive. The string tension was small and was considered negligible to the test.

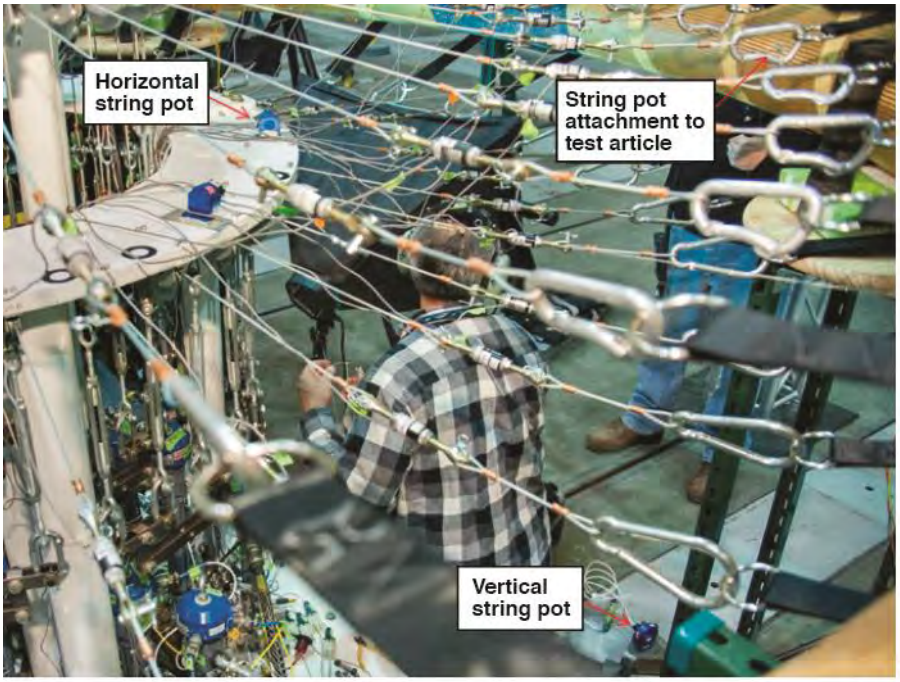

Figure 24. String displacement potentiometer transducer locations.

6.2 Liquid Metal Strain Gages

Sixteen liquid metal strain gages (LMSGs) were installed at various locations on the upper and lower cords of each test article. These highly flexible indium-gallium-filled silicon tube strain gages were used to provide the ability to measure the potentially large strain values of the test articles. Unlike conventional ridged sensors, the highly elastic instrumentation provided minimal effect on the test article material. The LMSG bonding to the chords was achieved by using Dow Corning® 3145 silicon adhesive (Dow Corning Corporation, Auburn, Michigan) while the test article was pressurized at 2 psi. To prevent damage to the LMSGs when the test article is fully deflated, the instrumentation was slightly pre-strained prior to bonding. Figure 25 shows a typical LMSG installation and Figure 26 shows the distribution of LMSGs on each test article.

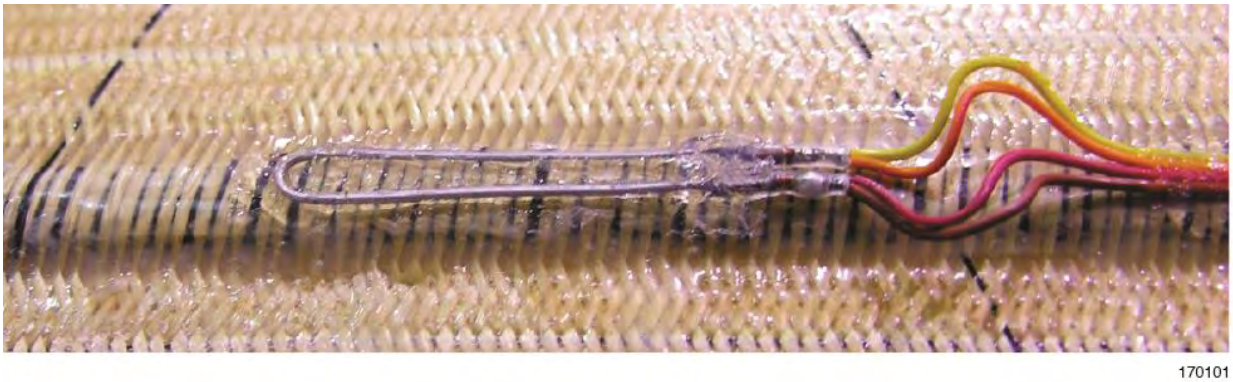

Figure 25. Close-up view of a liquid metal strain gage installed on the test article.

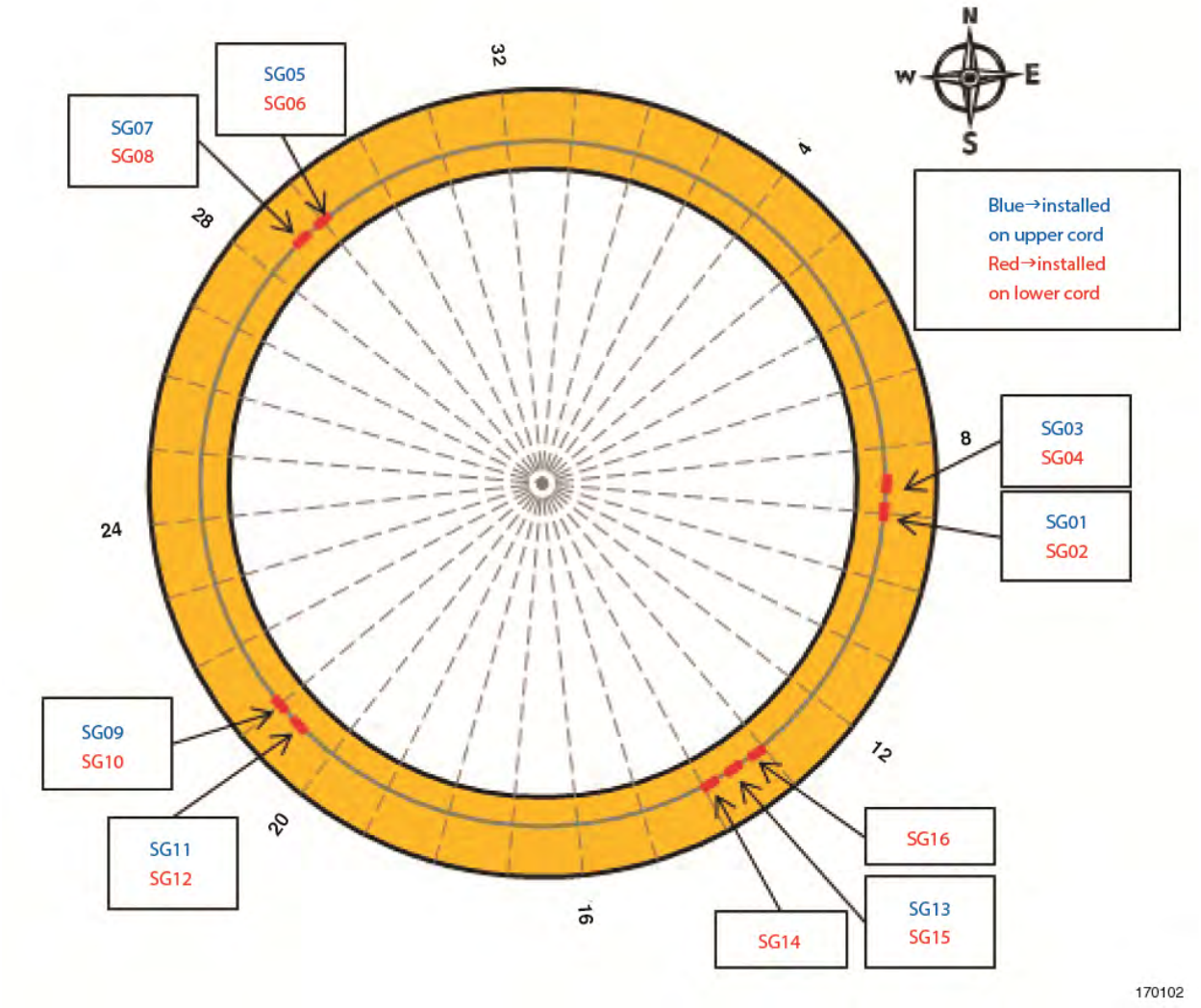

Figure 26. Liquid metal strain gage installation locations.

6.3 The PONTOS Displacement Measurement System

A PONTOS photogrammetry system was used to measure the global spatial displacement of each test article during load testing. The PONTOS system model #TXG50-K06 (GOM Optical Measuring Techniques, Braunschweig, Germany) was used, which is a non-contact, optical, 3-D point-tracking measurement system. The purpose of this system was to capture global movement of the test article during test by measuring the spatial position of targets located on the surface of each test article (figure 27), using two cameras looking down onto the test article from a height of approximately 20 ft (figure 28 and figure 29). Depending on the size of the test article, 80 to 120 targets were placed on the upper surface of the test article. There were also additional targets placed on stationary structures serving as reference points. The PONTOS data was taken at a rate of 1 image per second.

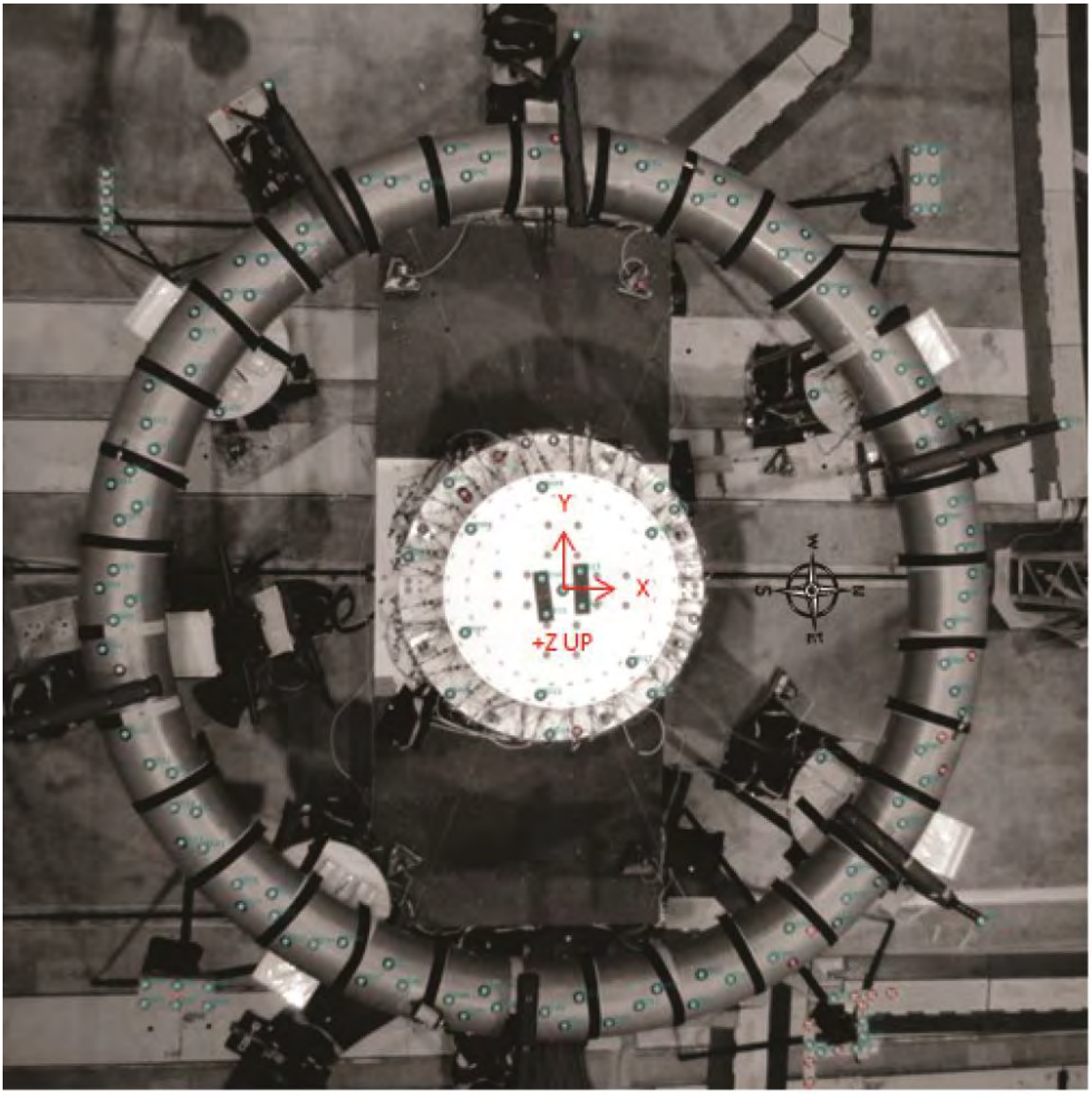

Figure 27. A PONTOS camera view showing a target installed on test article T3A-4.

Figure 28. The setup of the PONTOS cameras.

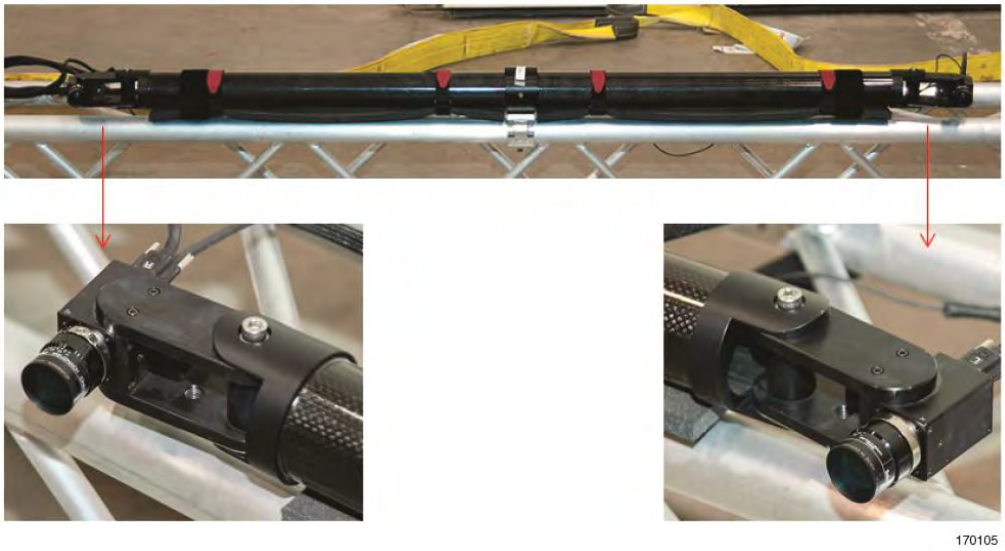

Figure 29. The PONTOS cameras as installed on the truss frame.

6.4 The ARAMIS Strain Measurement System

An ARAMIS photogrammetry system was also used to measure the full-field strain map of a portion of each test article during load testing. The ARAMIS photogrammetry system (GOM Optical Measuring Techniques, Braunschweig, Germany) is a dynamic, 3-D surface-strain measurement system that captured strains of a surface region as the test article was being loaded. The ARAMIS data collection field was focused at an inner radius region between two straps (see figure 30). Instead of targets, ARAMIS used a stochastic or random pattern that was painted on the test article. The measurement locations were different between test articles (see table 2). Initially, the ARAMIS pattern was overlapped on top of three LMSGs (LMSGs SG14, SG15, and SG16) for direct data comparison. Later, the pattern was moved away from these LMSGs so that the strain images without the instrumentation wirings could look smoother. The ARAMIS data were taken at a rate of six images per second.

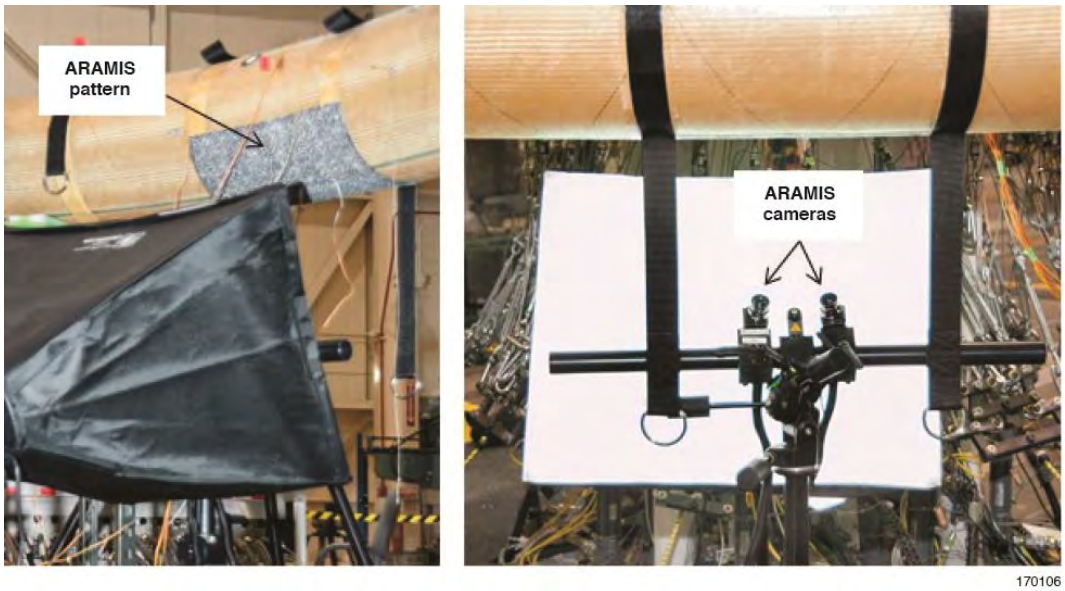

Figure 30. The ARAMIS cameras and pattern.

Table 2. The ARAMIS pattern location on each test article.

Test Article	Pattern Location
T3A-4	Between straps 15 & 16, lower cord
T4A-1	Between straps 15 & 16, lower cord
T4A-2	Between straps 15 & 16, lower cord
T4A-3	Between straps 15 & 16, lower cord
T5A-1 (Sep 2013)	Between straps 13 & 14, lower cord
T5A-1 (Feb 2014)	Between straps 28 & 29, lower & upper cords
T5B-1	Between straps 15 & 16, lower cord
T5B-2	Between straps 15 & 16, lower cord
T5C-1	Between straps 13 & 14, lower cord

6.5 Tension Load Link (In-Line Load Cell)

Sixty-four in-line load cells were installed in the horizontal part of the load trains between the pulleys and the test article D-rings (figure 31). The in-line load cells were required in addition to the load control load cells installed on the hydraulic jacks because the pulley system introduced friction loss to the applied loads. The in-line load cells provided direct measurement of the loads being applied to the test article. Figure 32 shows the distribution and channel names for all the in-line load cells.

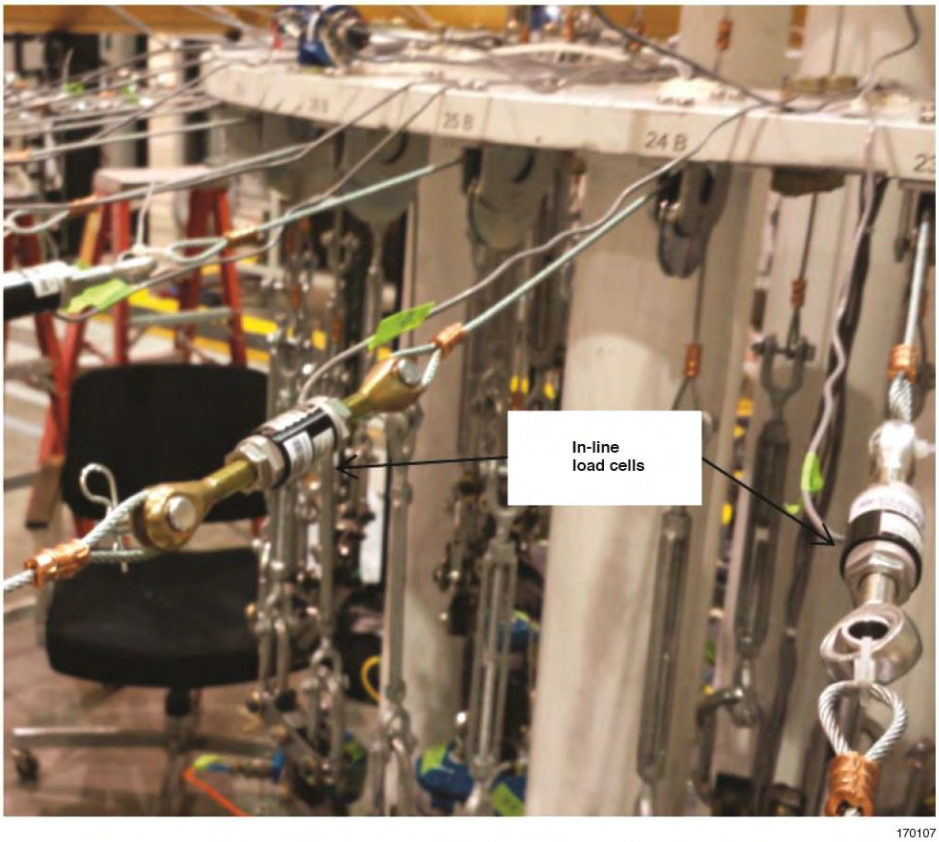

Figure 31. In-line load cell as installed in the load train.

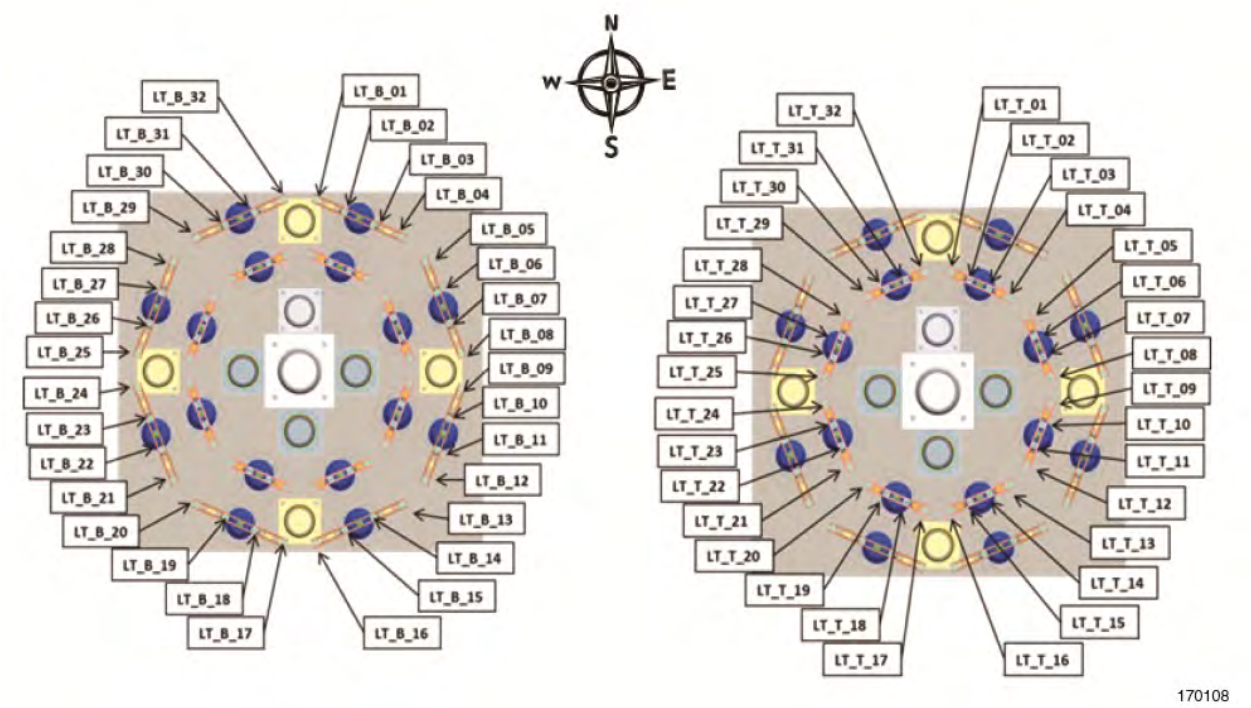

Figure 32. In-line load cell distribution and channel names.

6.6 Control Load Cell

A low-profile load cell was installed on top of each hydraulic jack to measure the applied load. These 16 load cells provided feedback to the MLCS to ensure the commanded loads were being properly applied. Figure 33 shows a typical load cell installation and figure 34 shows the locations of the load cells in the test setup.

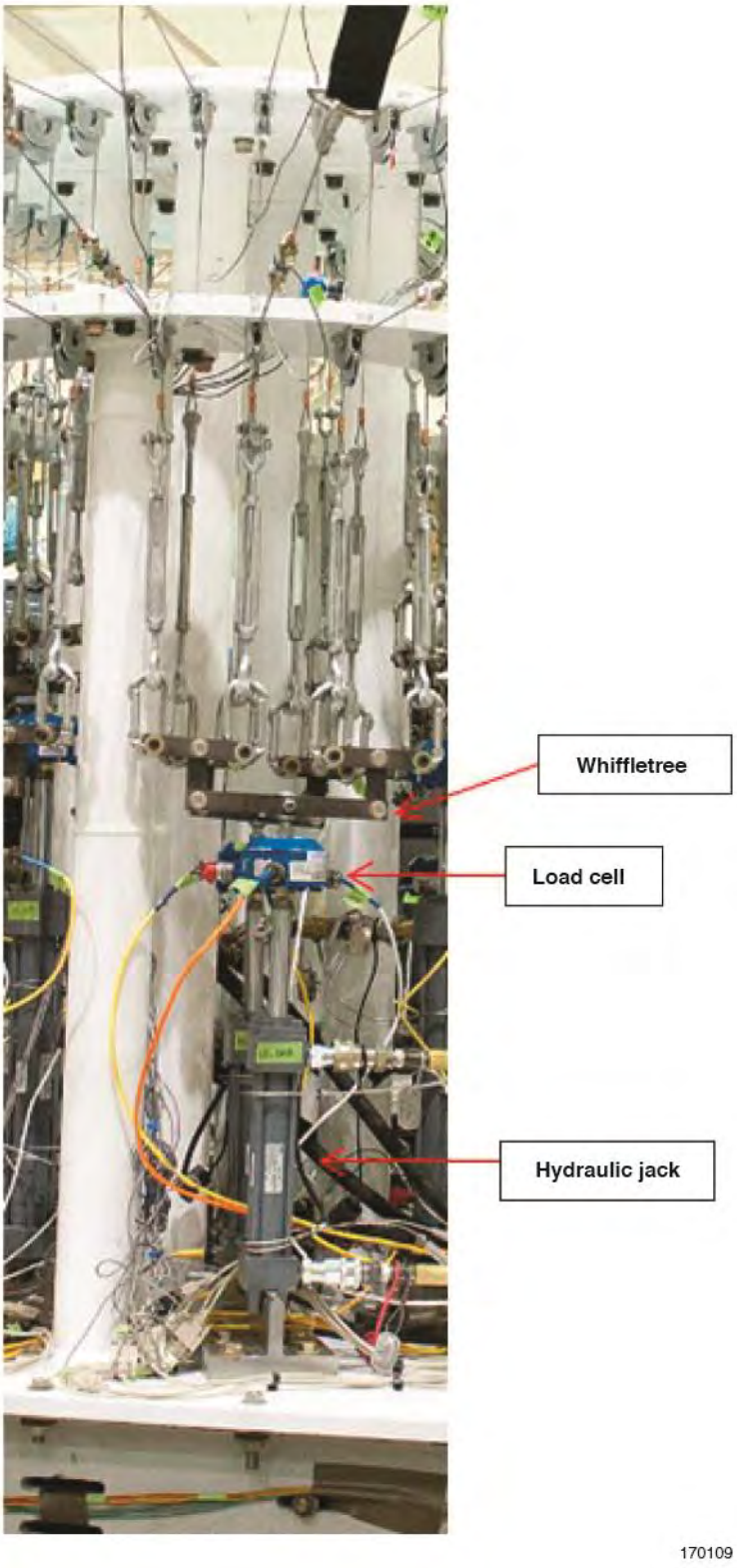

Figure 33. A typical control load cell installed in the load train.

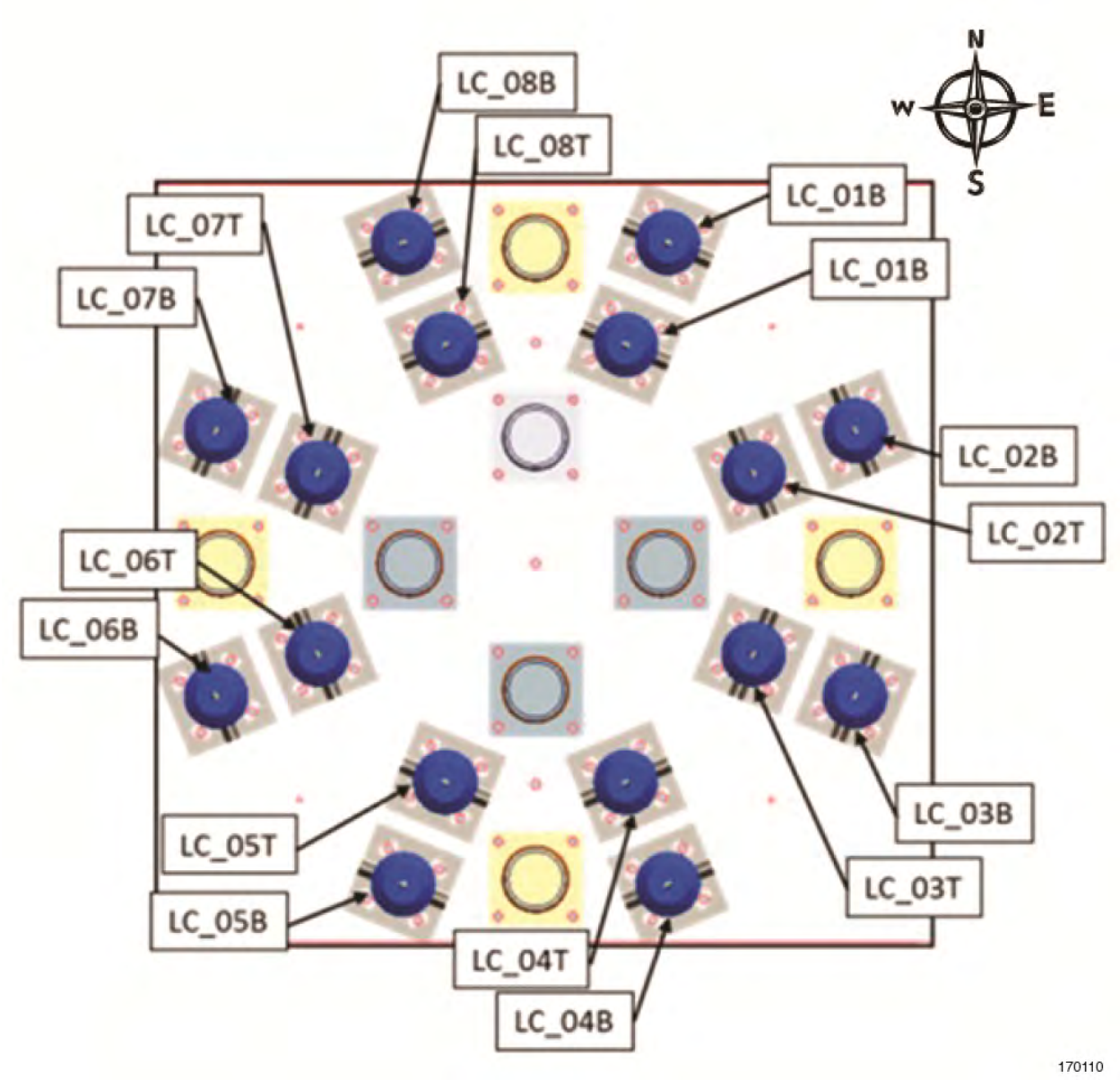

Figure 34. Top view of control load cell measurement locations.

6.7 Pressure Transducer

A pressure transducer was installed on one of the four ports to monitor the test article pressure. A second port was used for inflation and deflation while the remaining two ports were plugged and were not used.

6.8 Thermocouple

Test area temperature was measured by a thermocouple for post-test data analysis, as temperature variation had a slight effect on test article pressure and strain gage measurements.

6.9 Hydraulic Jack Stroke

Each hydraulic jack had a built-in linear resistance transducer (LRT) that output the jack stroke to the test data system. The 16 LRT (figure 35) data channels were also monitored and recorded during testing.

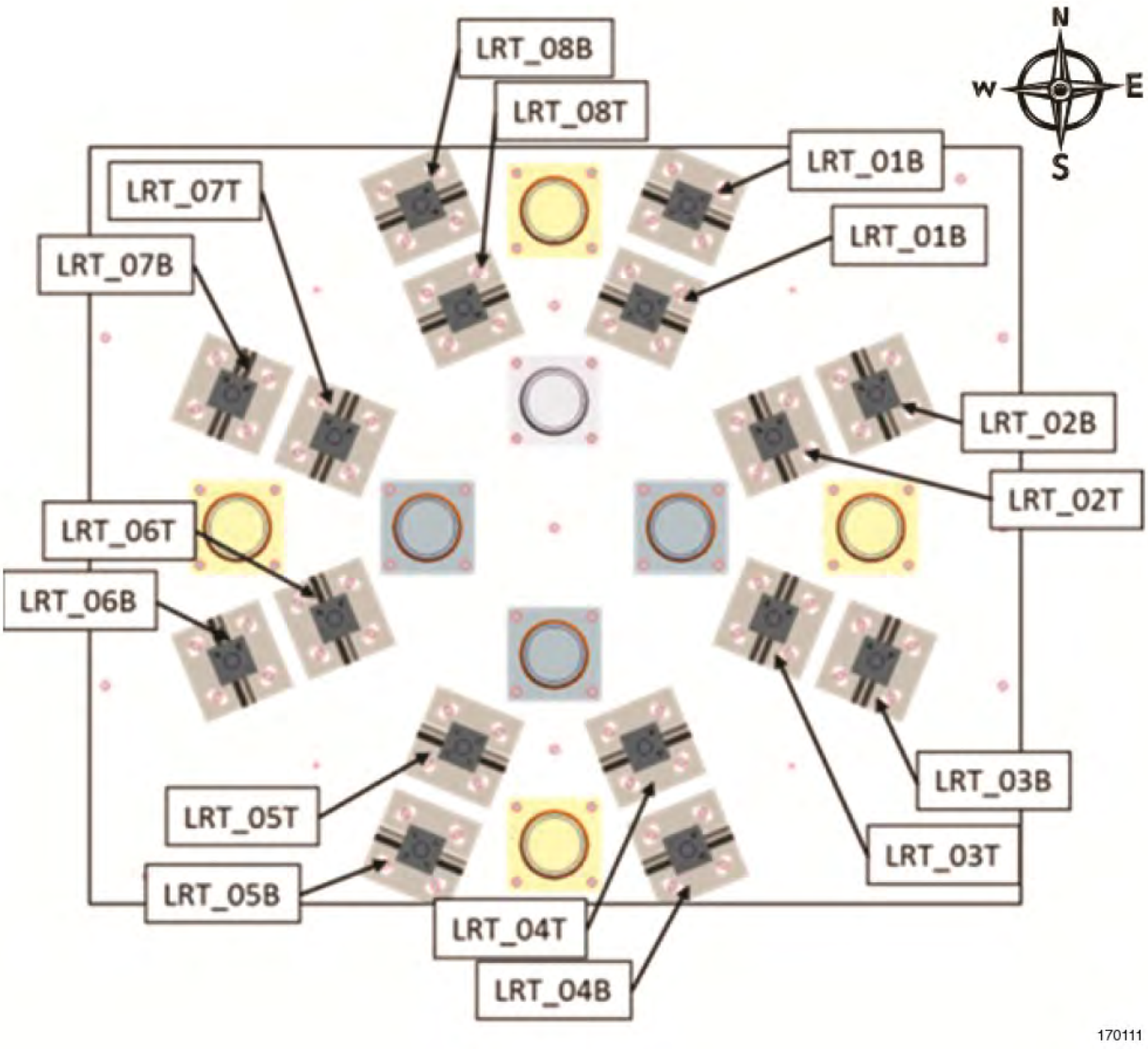

Figure 35. Top view of jack stroke measurement locations.

6.10 Video

Test videos (figure 36) were captured using five cameras. These cameras were set up to monitor the test article and the test setup from different angles and zoom settings. The video display allowed the testing personnel both in the control room and at NASA LaRC to visually observe the test in real time.

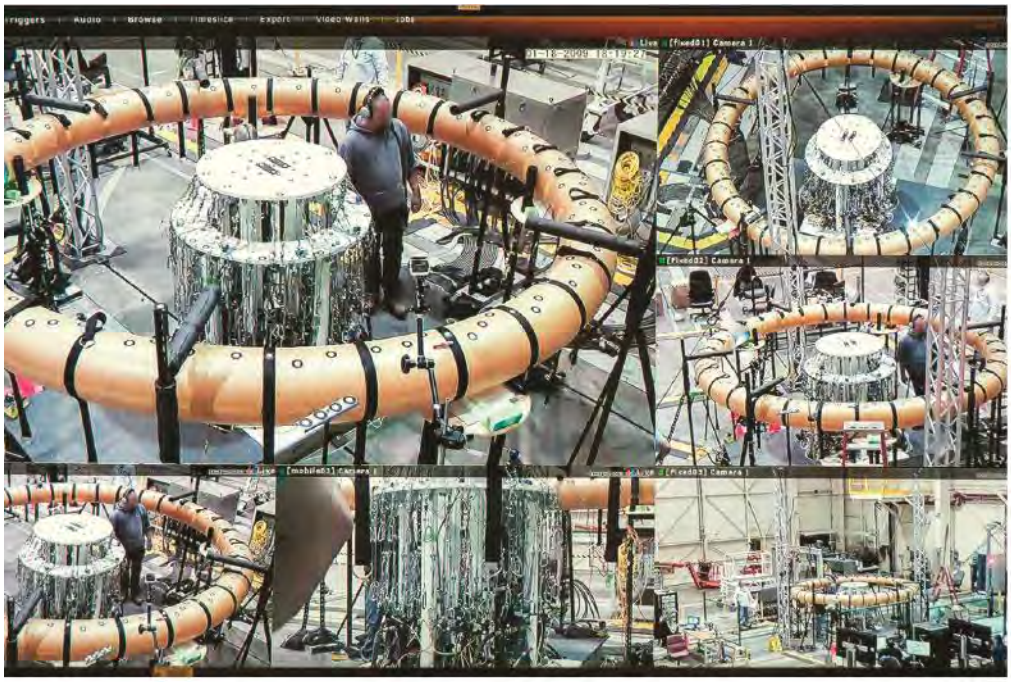

Figure 36. A typical video display during testing.

In additional to the FLL video, photographs and videos of some portions of the tests were taken by the AFRC photographer and videographer.

6.11 Go / No Go Instrumentation

Go / No-Go instrumentation was defined prior to the beginning of testing: Parameters that were determined and required to be in operational to both safely execute the tests and to achieve the objectives of the tests. The Go / No Go instrumentation was:

- the pressure transducer,
- six of the eight horizontal string displacement potentiometers (the two non-working string pots cannot be adjacent to each center),
- all 16 load control and 64 in-line load cells,
- the ARAMIS photogrammetry system,
- the PONTOS photogrammetry system, and
- 16 LRTs.

6.12 Data Acquisition System

Instrumentation data were recorded using the FLL data acquisition system (DAS) with the exception of the photogrammetry data. The string pot, LMSG, LRT, and load cell data were recorded at 20 samples per second during loading. This rate was relaxed to 4 samples per second between test points to save data space. The Interactive Analysis and Display System® (IADS®) (Symvionics Inc, Arcadia, California) was used and programmed to show the DAS data in various types of charts for real-time monitoring.

7.0 Pre-Test Preparation

From the time the test article arrived in the FLL to the start of testing, several tasks needed to be performed in order to prepare the test article and the test setup.

When each test article was delivered to the FLL, it was first visually inspected for damage incurred during shipping. If no damage was found, the article was inflated to 2 psi for additional inspection and strap number marking. The seam at which the fabric of the test article joined was defined as the west side of the article with respect to the FLL, and the side having the inflation port was defined as the top side. Starting at the north side of the test article, strap numbers 1 through 32 were marked on the test article in the clockwise direction as shown in figure 4. After the straps had been labeled, LMSGs and the ARAMIS pattern could then be installed (figure 37). The installation process usually took approximately four days.

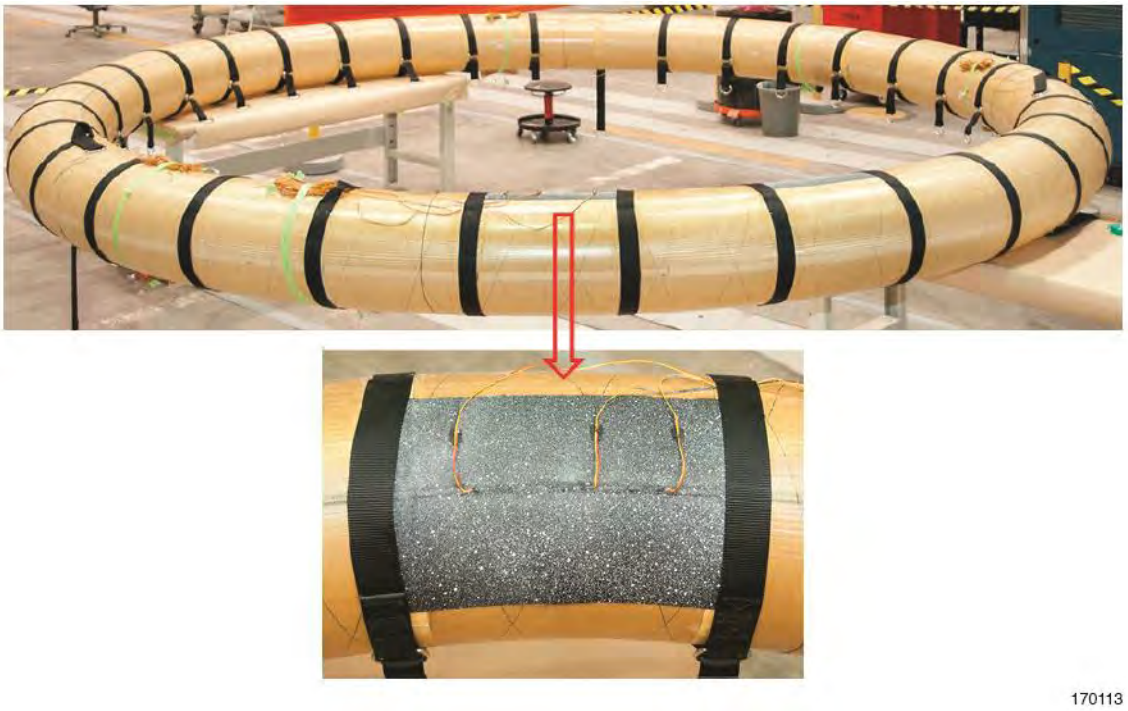

Figure 37. Liquid metal strain gages and the ARAMIS pattern installed on the test article.

After completion of the installation process described above, the test article was ready to be placed in the test setup (figure 38). Once the test article was placed on the test stands and centered to the hub stand, all of the load train lengths and the string pot lengths could be fine-tuned to ensure there would be enough length to accommodate test article deformation. The photogrammetry PONTOS targets were also placed on the test article at this time. After the PONTOS targets were in place and the PONTOS system calibrated, the test article was then inflated to 15 psi for pre-test braid angle measurements. The ARAMIS system was then put in place and the calibration was performed. Figure 39 shows the test article in test configuration (placed on the test stands and connected to the load trains).

170114

Figure 38. Flight Loads Laboratory technicians placing the test article in the test setup.

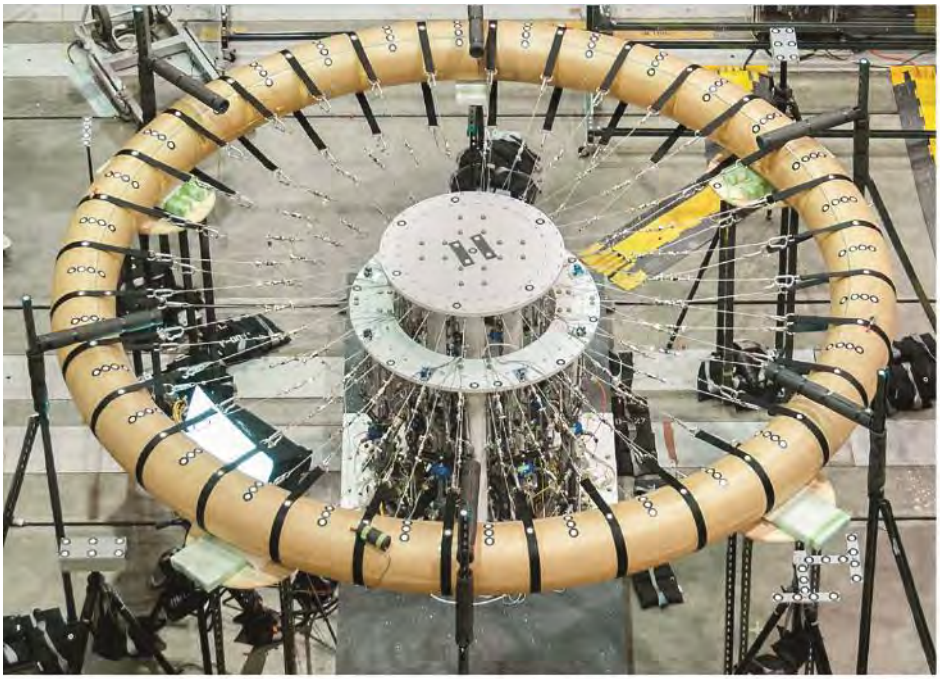

170115

Figure 39. The test article in test configuration.

8.0 Testing

Torus testing required a number of systems to be functioning properly and many operations to be executed correctly in order to successfully achieve the test objectives. An all-inclusive procedures checklist was used to ensure that testing was performed in an efficient and safe manner. Notable test events and observations are summarized in the following sections.

8.1 Execution of Test

On test days, once instrumentation systems had been warmed up, pressure cycles were initiated to reduce the test article response hysteresis (see section 8.3.3, "Benefits of Pre-test Pressure Cycles," for more detail). Pressure-cycling usually took one to two hours, depending on the number of cycles required. Immediately following was a crew brief, before all test personnel proceeded to their assigned stations. At each station, functional verifications were performed for the IADS® displays, instrumentation systems, and the hydraulics system. Mechanics then connected the load trains, including hooking the load cables to the strap-ends. Once the pre-loads had been applied and all load trains visually verified to be in the proper configuration, the load profile was initiated. When the test article buckled, the MLCS was taken out of load control mode and put into position control, and all of the hydraulic jacks held position for a few seconds to allow data collection of the buckled shape. The hydraulic jacks then were extended to the no-load positions to prepare for either another load cycle or test shutdown. When all tests were completed for the day, the shutdown section of the checklist was executed, which included disconnecting the load cables from the test article, de-pinning the whiffletrees from the load cells, and deflating the test article from test pressure to 2 psi. Test data then were transferred to the FLL data server for post-test processing.

8.2 Test Summary

Overall, the testing was successful because the test objectives were met. As the test team gained new information about the behavior of the test articles, however, a few load cases were removed from the test matrix because buckling was assumed to be either unattainable or not useful for FEM validation. The following sections discuss the test events in detail.

8.2.1 Test Setup Checkout

Prior to the actual start of the tests, checkout operations were conducted to verify the readiness of the test setup. Checkout operations involved pressure-cycling the test article between 2 psi and 20 psi while monitoring the instrumentation output. The checkout operations provided an opportunity to exercise the instrumentation without activating the hydraulics - a low-risk approach to ensuring the success of the test. The checkout operations also allowed the test team to become familiarized with the checklist execution and the IADS® displays.

These operations helped in verifying whether the instrumentation was working properly. It was also observed that a few pressure cycles were required to pre-condition the test article for testing, which requirement was not expected during test planning. The need for pre-conditioning the test article was observed in the hysteresis revealed in the LMSG data (see section 8.3.3, "Benefits of Pre-Test Pressure Cycles"). Thus the checklist was modified to conduct up to three pressure cycles at the beginning of each day of testing.

8.2.2 Test Article T5C-1

The T5C-1 test article was the first test article tested. The first test case was compression loading at 20 psi. The buckling loads for the first three test runs were between 233 lbf and 238 lbf, while the estimated buckling load range was 320 lbf to 400 lbf, as shown in the table A-1 entry for load case LC 1C. Since the

buckling loads were considerably different than the estimated values, the test team decided that future torsion load profiles shall be updated based on the compression test results.

After both compression and torsion tests at 20 psi had been completed, a data review was conducted to verify that the instrumentation setup for data collection was sufficient to capture the response of the test article. The result of the review indicted that the data collection was satisfactory in meeting the test objectives; no instrumentation change was required.

The buckling loads for the 10-psi tests being lower than expected, it was decided that the 5-psi tests would not yield useful data and were therefore not performed.

Table 3 shows a summary of the test performed for the T5C-1 test article. Since instrumentation zeroing was performed before the load distributing whiffletrees were attached to the hydraulic jacks, the whiffletree weight of 10 lb needed to be added to the jack load listed in the "Applied Loads" columns when trying to determine the total applied load on the test article. A total of 18 compression and torsion tests runs were completed at various test pressures.

Table 3. Summary of testing of the T5C-1 test article.

Test Article Outer Diameter = 15'								
Test Number	Date	Load Case	Test Article Pressure	Applied Loads		Ramp Rate	Buckling Loads	
				Ramp-Up	Target Load		Average Jack Load for Top Load Trains (LCT)	Average Jack Load for Bottom Load Trains (LCB)
			(psi)	(lbf)	(lbf)	(lbf/sec)	(lbf)	(lbf)
1	8/15/2013	LC 1C	20	-	1590	10	238	238
2	8/15/2013	LC 1C	20	-	1590	10	234	234
3	8/15/2013	LC 1C	20	-	1590	10	233	233
4	8/15/2013	LC 1T	20	130	250	10	Did Not Buckle	
5	8/15/2013	LC 1T	20	190	370	10	248	132
6	8/15/2013	LC 1T	20	190	370	10	240	139
7	8/16/2013	LC 1T	20	190	370	10	246	134
8	8/16/2013	LC 1T	20	190	370	10	242	138
9	8/20/2013	LC 1C	20	-	1590	60*	245	246
10	8/20/2013	LC 1C	20	-	1590	10	234	235
11	8/27/2013	LC 2C	15	-	1590	10	179	180
12	8/27/2013	LC 2C	15	-	1590	10	173	174
13	8/27/2013	LC 2T	15	143	276	5,2**	181	103
14	8/27/2013	LC 2T	15	143	276	5,2**	180	105
15	8/28/2013	LC 3C	10	-	1590	5	116	115
16	8/28/2013	LC 3C	10	-	1590	5	110	111
17	8/28/2013	LC 3T	10	90	180	5,2**	118	64
18	8/28/2013	LC 3T	10	90	180	5,2**	116	66

* Ramp rate was erroneously set high

** Ramp rates set low to allow photogrammetry systems to capture more data in torsion case.
(5 Lbf/Sec to Ramp-Up Load and 2 Lbf/Sec to Reference Load)

8.2.3 Test Article T5A-1

The T5A-1 test article was the same size as, but had a different braid angle compared to, test article T5C-1 and had much higher predicted bucking loads than T5C-1. Table 4 shows a summary of the test performed for the T5A-1 test article. A total of seven compression test runs were completed at 20 psi. During the first three compression tests at 20 psi, it was observed that the buckling loads were indeed higher than those of the T5C-1 test article; however, during these three repeated tests the buckling loads had a significant decreasing pattern from 612 lbf down to 541 lbf, eventually ending up at 507 lbf. As well, while disconnecting the straps from the load cables, it was observed that strap #2 had de-bonded from the test

article. Testing was put on hold for several days until the necessary adhesive was received in the FLL and strap #2 re-bonded to the test article.

Table 4. Summary of first testing of the T5A-1 test article.

Test Article Outer Diameter = 15'								
Test Number	Date	Load Case	Test Article Pressure	Applied Loads		Ramp Rate	Buckling Loads	
				Ramp-Up	Target Load		Average Jack Load for Top Load Trains (LCT)	Average Jack Load for Bottom Load Trains (LCB)
			(psi)	(lbf)	(lbf)	(lbf/sec)	(lbf)	(lbf)
19	9/6/2013	LC 5C	20	-	1590	10	611	612
20	9/6/2013	LC 5C	20	-	1590	10	540	541
21	9/6/2013	LC 5C	20	-	1590	10	506	507
22	9/17/2013	LC 5C	20	-	1590	10	448	448
23	9/17/2013	LC 5C	20	-	1590	10	389	389
24	9/30/2013	LC 5C	20	-	1590	10	448	447
25	9/30/2013	LC 5C	20	-	1590	10	379	379

When testing resumed, the same 20-psi compression tests were repeated to see if buckling loads would continue to decrease. As it turned out, the buckling loads for the 2 runs decreased from 448 lbf to 389 lbf. At this point, testing stopped because there was a concern that the decreasing buckling loads were due to damage incurred to the test article during the initial buckling event.

The NASA LaRC requested that the test article manufacturer, HDT Global (Solon, Ohio), send personnel to the FLL to inspect the test article. On-site inspection of the test article did not detect any structural damage, however, the HDT Global representative suggested that some braid manipulation work be done to re-align the braids back to the as-manufactured angle.

After the braid manipulation work was completed, the test article went through two more compression runs at 20 psi. Once again, the buckling loads decreased significantly from 448 lbf to 379 lbf. At this point the test team decided to stop testing and send the test article to HDT Global for a detailed inspection. The detailed inspection did not discover any damage to the test article. The manufacturer again re-aligned the braid angles and sent the test article back to AFRC for re-testing. The re-testing is discussed in section 8.2.8, “Test Article T5A-1 Re-Test.”

In order to obtain smoother ARAMIS data images, a review of the ARAMIS and LMSG data at their overlapped area was performed and the team was able to validate the accuracy of the LMSG data. The test team then was able to place the ARAMIS pattern at other locations rather than on top of the three LMSGs. For the remainder of the test program, the ARAMIS pattern was placed in a location other than on top of the three LMSGs between straps 13 and 14 (see table 2).

At this point, the NASA LaRC suggested decreasing the loading ramp rate from 10 lbf per second to 5 lbf per second to allow photogrammetry systems to capture more data. The test team also decided to add the eight vertical string pot measurements at the same locations where the horizontal string pots attached to the test article. This method would provide out-of-plane displacement data in real time to help identify buckling initiation.

8.2.4 Test Article T4A-1

For the testing of test article T4A-1, the test team decided to conduct torsion tests first to see if experiencing torsional loads first would change the response of the test article. Unlike the compression load profile, which was a steadily increasing load for all the load trains until buckling occurred, the applied load for the bottom load trains in the torsion load profile was a steadily decreasing load that had to stop when the minimum tension load was reached (see figure 8). Therefore, the torsion profiles required a close estimation of the buckling loads. If the ramp-up load were set too high, then the test article would buckle

before the load profile reached the ramp-up load. The ramp-up load was the initial compression load applied to the test article. If the ramp-up and the target loads were set too low, then the test article would not buckle.

During torsion test runs numbered 26 and 27, the test article did not buckle because the ramp-up and target loads were set too low, however, after reprogramming the torsion load profiles to higher values, the test team was able to successfully buckle the test article.

Initial test runs for torsion at 15 psi did not result in buckling. Additional tests at higher applied loads could have been run, however, due to time constraints, they were not performed.

Table 5 shows a summary of the testing performed for the T4A-1 test article. A total of 19 compression and torsion test runs were completed at various test pressures.

Table 5. Summary of testing of the T4A-1 test article.

Test Article Outer Diameter = 13'								
Test Number	Date	Load Case	Test Article Pressure	Applied Loads		Ramp Rate	Buckling Loads	
				Ramp-Up	Target Load		Average Jack Load for Top Load Trains (LCT)	Average Jack Load for Bottom Load Trains (LCB)
			(psi)	(lbf)	(lbf)	(lbf/sec)	(lbf)	(lbf)
26	10/29/2013	LC 9T	20	385	760	5	Did Not Buckle	
27	10/29/2013	LC 9T	20	385	760	5	Did Not Buckle	
28	10/30/2013	LC 9T	20	510	1010	5	821	192
29	10/30/2013	LC 9T	20	510	1010	5	785	226
30	10/30/2013	LC 9T	20	510	1010	5	498	498
31	10/30/2013	LC 9T	20	510	1010	5	475	475
32	11/4/2013	LC 9T	20	510	1010	5	510	510
33	11/4/2013	LC 10C	15	-	< 1590	5	436	436
34	11/4/2013	LC 10C	15	-	< 1590	5	385	386
35	11/4/2013	LC 10T	15	250	490	5	Did Not Buckle	
36	11/4/2013	LC 10T	15	250	490	5	Did Not Buckle	
37	11/5/2013	LC 11C	10	-	< 1590	5	366	366
38	11/5/2013	LC 11C	10	-	< 1590	5	324	324
39	11/5/2013	LC 11T	10	250	490	5	401	96
40	11/5/2013	LC 11T	10	250	490	5	394	101
41	11/5/2013	LC 12C	5	-	< 1590	5	190	191
42	11/5/2013	LC 12C	5	-	< 1590	5	185	185
43	11/7/2014	LC 12T	5	145	280	5	196	92
44	11/7/2014	LC 12T	5	145	280	5	194	93

8.2.5 Test Article T4A-3

Due to its construction utilizing cords of weaker strength, test article T4A-3 had a lower maximum operating pressure. The highest test pressure for the T4A-3 test article was limited to 15 psi.

Near the end of the first day of testing, FLL test personnel noticed a small bulge (see figure 40) on the fabric between straps 24 and 25 near the seam of the braid fabric. Suspecting that this bulge was the result of mechanical loading, testing was suspended to allow evaluation of the test article. It was not clear whether the bulge had been present prior to the first test run of test article T4A-3.

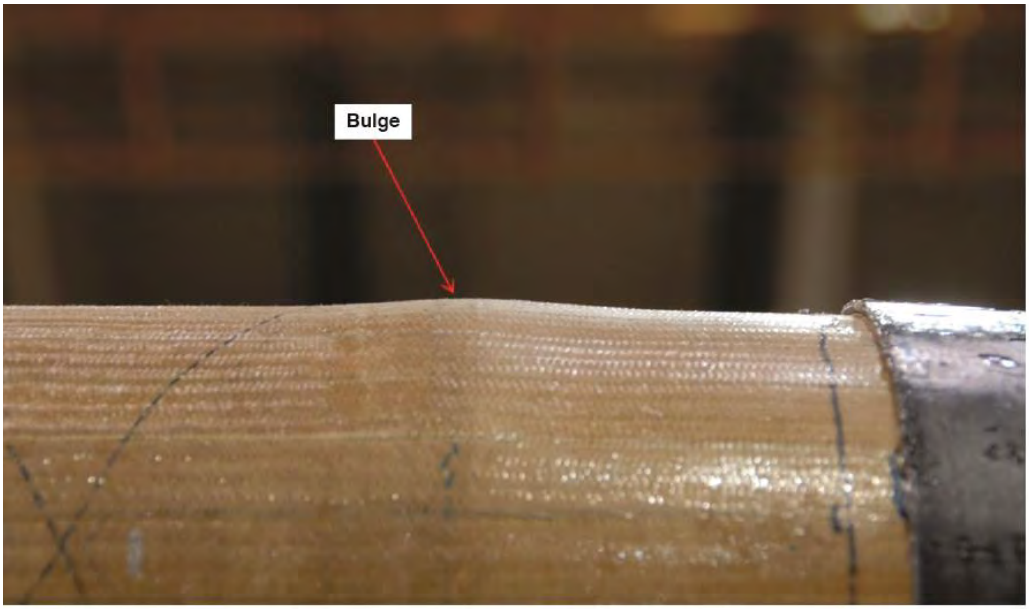

Figure 40. Bulge on test article T4A-3.

Upon further examination of test article T4A-3 and other test articles, it was believed that the bulge had been created during manufacturing. Testing resumed, with close visual monitoring of the bulge. The size of the bulge appeared to remain the same for the remaining tests conducted on test article T4A-3.

Table 6 shows a summary of the testing performed for the T4A-3 test article. A total of 15 compression and torsion test runs were completed at various test pressures.

Table 6. Summary of testing of the T4A-3 test article.

Test Article Outer Diameter = 13'								
Test Number	Date	Load Case	Test Article Pressure	Applied Loads		Ramp Rate	Buckling Loads	
				Ramp-Up	Target Load		Average Jack Load for Top Load Trains (LCT)	Average Jack Load for Bottom Load Trains (LCB)
			(psi)	(lbf)	(lbf)	(lbf/sec)	(lbf)	(lbf)
45	11/13/2013	LC 17C	15	-	< 1590	5	459	459
46	11/13/2013	LC 17C	15	-	< 1590	5	379	379
47	11/13/2013	LC 17C	15	-	< 1590	5	347	347
48	11/13/2013	LC 17T	15	270	531	5	Did Not Buckle	
49	11/15/2013	LC 17T	15	310	610	5	567	66
50	11/15/2013	LC 17T	15	310	610	5	573	62
51	11/15/2013	LC 17T	15	310	610	5	568	67
52	11/15/2013	LC 18C	10	-	< 1590	5	313	313
53	11/15/2013	LC 18C	10	-	< 1590	5	291	291
54	11/15/2013	LC 18T	10	237	463	5	381	87
55	11/15/2013	LC 18T	10	237	463	5	384	84
56	11/18/2013	LC 19C	5	-	< 1590	5	191	192
57	11/18/2013	LC 19C	5	-	< 1590	5	187	188
58	11/18/2013	LC 19T	5	153	296	5	209	92
59	11/18/2013	LC 19T	5	153	296	5	204	95

8.2.6 Test Article T4A-2

The T4A-2 test article was identical to the T4A-1 test article. The purpose of testing these two identical test articles was to demonstrate and verify repeatability. Overall, the buckling loads for both test articles were close, as shown in table 5 and table 7. Test run number 61 was intended to be a torsion test, but the test article buckled before reaching the ramp-up load. This test was therefore considered to be a compression test, and the same loading was repeated three times to complete the compression test at 20 psi.

Table 7 shows a summary of the testing performed for the T4A-2 test article. A total of 21 compression and torsion test runs were completed at various test pressures.

Table 7. Summary of testing of the T4A-2 test article.

Test Article Outer Diameter = 13'								
Test Number	Date	Load Case	Test Article Pressure	Applied Loads		Ramp Rate	Buckling Loads	
				Ramp-Up	Target Load		Average Jack Load for Top Load Trains (LCT)	Average Jack Load for Bottom Load Trains (LCB)
			(psi)	(lbf)	(lbf)	(lbf/sec)	(lbf)	(lbf)
60	11/20/2013	LC 13T	20	510	1010	5	780	236
61	11/20/2013	LC 13C	20	510	1010	5	453	452
62	11/20/2013	LC 13C	20	510	1010	5	447	447
63	11/20/2013	LC 13C	20	510	1010	5	448	448
64	11/20/2013	LC 13T	20	350	690	5	690	10
65	11/20/2013	LC 13T	20	350	690	5	Did Not Buckle	
66	11/20/2013	LC 13T	20	395	780	5	750	42
67	11/20/2013	LC 13T	20	395	780	5	673	113
68	11/21/2013	LC 14C	15	-	< 1590	5	389	391
69	11/21/2013	LC 14C	15	-	< 1590	5	370	371
70	11/21/2013	LC 14T	15	333	656	5	579	84
71	11/21/2013	LC 14T	15	333	656	5	565	98
72	11/21/2013	LC 15C	10	-	< 1590	5	312	311
73	11/21/2013	LC 15C	10	-	< 1590	5	293	294
74	11/21/2013	LC 15T	10	259	508	5	257	257
75	11/21/2013	LC 15T	10	220	430	5	396	40
76	11/21/2013	LC 15T	10	220	430	5	373	65
77	11/22/2013	LC 16C	5	-	< 1590	5	190	190
78	11/22/2013	LC 16C	5	-	< 1590	5	188	188
79	11/22/2013	LC 16T	5	145	280	5	197	90
80	11/22/2013	LC 16T	5	145	280	5	197	90

8.2.7 Test Article T3A-4

The T3A-4 test article was the smallest test article. Prior to testing, some load train hardware was replaced in order to reduce the load trains to the proper lengths.

Table 8 shows a summary of the testing performed for the T3A-4 test article. A total of 18 compression and torsion test runs were completed at various test pressures.

Table 8. Summary of testing of the T3A-4 test article.

Test Article Outer Diameter = 11'								
Test Number	Date	Load Case	Test Article Pressure	Applied Loads		Ramp Rate	Buckling Loads	
				Ramp-Up	Target Load		Average Jack Load for Top Load Trains (LCT)	Average Jack Load for Bottom Load Trains (LCB)
			(psi)	(lbf)	(lbf)	(lbf/sec)	(lbf)	(lbf)
81	1/22/2014	LC 20C	20	-	< 1590	5	777	777
82	1/22/2014	LC 20C	20	-	< 1590	5	692	692
83	1/22/2014	LC 20C	20	-	< 1590	5	636	636
84	1/22/2014	LC 20T	20	487	964	5	812	158
85	1/22/2014	LC 20T	20	487	964	5	797	171
86	1/22/2014	LC 20T	20	487	964	5	796	172
87	1/23/2014	LC 21C	15	-	< 1590	5	579	579
88	1/23/2014	LC 21C	15	-	< 1590	5	556	556
89	1/23/2014	LC 21T	15	427	844	5	602	246
90	1/23/2014	LC 21T	15	427	844	5	598	250
91	1/23/2014	LC 22C	10	-	< 1590	5	387	387
92	1/23/2014	LC 22C	10	-	< 1590	5	380	380
93	1/23/2014	LC 22T	10	295	580	5	388	197
94	1/23/2014	LC 22T	10	295	580	5	385	202
95	1/24/2014	LC 23C	5	-	< 1590	5	188	189
96	1/24/2014	LC 23C	5	-	< 1590	5	184	185
97	1/24/2014	LC 23T	5	148	286	5	196	92
98	1/24/2014	LC 23T	5	148	286	5	189	103

8.2.8 Test Article T5A-1 Re-Testing

After a thorough inspection of the T5A-1 test article by the manufacturer, which found no damage, the T5A-1 test article was re-tested at 20 psi and the other test pressures specified in the test matrix. The results of the tests indicated that the buckling loads still had the decreasing pattern and that the refurbishment work seemed to have minimal effect with helping the test article to maintain consistent buckling loads.

At 15 psi, the test article did not buckle in torsion although the applied loads had been increased three times from test run number 106 to test run number 109. After test run number 109, it was decide not to continue with torsion testing because the ramp-up load of 276 lbf for test run number 109 was already very close to the buckling load for compression of 286 lbf. Further increase in the load profile would likely have resulted in buckling at ramp-up load and would have been identical to test run number 105.

Table 9 shows a summary of the testing performed for the re-testing of the T5A-1 test article. A total of 20 compression and torsion test runs were completed at various test pressures.

Table 9. Summary of re-testing of the T5A-1 test article.

Test Article Outer Diameter = 15'								
Test Number	Date	Load Case	Test Article Pressure	Applied Loads		Ramp Rate	Buckling Loads	
				Ramp-Up	Target Load		Average Jack Load for Top Load Trains (LCT)	Average Jack Load for Bottom Load Trains (LCB)
			(psi)	(lbf)	(lbf)	(lbf/sec)	(lbf)	(lbf)
99	2/5/2014	LC 5C	20	-	< 1590	5	418	418
100	2/5/2014	LC 5C	20	-	< 1590	5	354	354
101	2/5/2014	LC 5T	20	276	541	5	Did Not Buckle	
102	2/5/2014	LC 5T	20	315	620	5	Did Not Buckle	
103	2/5/2014	LC 5T	20	335	660	5	660	10
104	2/7/2014	LC 6C	15	-	< 1590	5	341	341
105	2/7/2014	LC 6C	15	-	< 1590	5	286	286
106	2/7/2014	LC 6T	15	227	445	5	Did Not Buckle	
107	2/7/2014	LC 6T	15	246	481	5	Did Not Buckle	
108	2/7/2014	LC 6T	15	266	522	5	Did Not Buckle	
109	2/7/2014	LC 6T	15	276	542	5	Did Not Buckle	
110	2/7/2014	LC 7C	10	-	< 1590	5	283	283
111	2/7/2014	LC 7C	10	-	< 1590	5	263	263
112	2/7/2014	LC 7T	10	236	463	5	Did Not Buckle	
113	2/7/2014	LC 7T	10	236	463	5	383	88
114	2/7/2014	LC 7T	10	236	463	5	236	236
115	2/10/2014	LC 8C	5	-	< 1590	5	193	194
116	2/10/2014	LC 8C	5	-	< 1590	5	190	190
117	2/10/2014	LC 8T	5	153	295	5	209	91
118	2/10/2014	LC 8T	5	153	295	5	206	92

8.2.9 Test Article T5B-1

The T5B-1 test article responded to mechanical loading in a unique way compared to all of the previously-tested articles. Rather than sustaining shape until buckling occurred, test article T5B-1 displayed a very noticeable deformation prior to buckling. In torsion test runs, it continued to deform during the ramp-up hold. The large test article deformations used up most of the available stroke in the hydraulic jacks. After the 15-psi tests, it was decided not to test at 10 psi and 5 psi because larger deformations were expected and would cause the hydraulic jacks to bottom out.

Table 10 shows a summary of the testing performed for the T5B-1 test article. A total of eight compression and torsion test runs were completed: three tests at 20 psi and five tests at 15 psi.

Table 10. Summary of testing of the T5B-1 test article.

Test Article Outer Diameter = 15'								
Test Number	Date	Load Case	Test Article Pressure	Applied Loads		Ramp Rate	Buckling Loads	
				Ramp-Up	Target Load		Average Jack Load for Top Load Trains (LCT)	Average Jack Load for Bottom Load Trains (LCB)
			(psi)	(lbf)	(lbf)	(lbf/sec)	(lbf)	(lbf)
119	2/11/2014	LC 24C	20	-	< 1590	5	214	214
120	2/11/2014	LC 24C	20	-	< 1590	5	238	238
121	2/11/2014	LC 24C	20	-	< 1590	5	226	226
122	2/18/2014	LC 25C	15	-	< 1590	5	224	223
123	2/18/2014	LC 25C	15	-	< 1590	5	217	217
124	2/18/2014	LC 25C	15	-	< 1590	5	209	209
125	2/18/2014	LC 25T	15	167	324	5	Did Not Buckle	
126	2/18/2014	LC 25T	15	188	366	5	188	188

8.2.10 Test Article T5B-2

The T5B-2 test article also had very noticeable deformations before buckling, however, due to its stronger cords the deformations were manageable such that all of the test cases were completed without any occurrence of hydraulic jacks bottoming out.

Table 11 shows a summary of the testing performed for the T5B-2 test article. A total of 19 compression and torsion test runs were completed at various test pressures.

Table 11. Summary of testing of the T5B-2 test article.

Test Article Outer Diameter = 15'								
Test Number	Date	Load Case	Test Article Pressure	Applied Loads		Ramp Rate	Buckling Loads	
				Ramp-Up	Target Load		Average Jack Load for Top Load Trains (LCT)	Average Jack Load for Bottom Load Trains (LCB)
			(psi)	(lbf)	(lbf)	(lbf/sec)	(lbf)	(lbf)
127	2/20/2014	LC 26C	20	-	< 1590	5	Did Not Buckle*	
128	2/20/2014	LC 26C	20	-	< 1590	5	370	370
129	2/20/2014	LC 26C	20	-	< 1590	5	341	341
130	2/20/2014	LC 26C	20	-	< 1590	5	336	336
131	2/20/2014	LC 26T	20	279	548	5	Did Not Buckle	
132	2/20/2014	LC 26T	20	279	548	5	521	36
133	2/20/2014	LC 26T	20	279	548	5	510	47
134	2/21/2014	LC 27C	15	-	< 1590	5	315	315
135	2/21/2014	LC 27C	15	-	< 1590	5	286	286
136	2/21/2014	LC 27T	15	239	468	5	405	68
137	2/21/2014	LC 27T	15	239	468	5	398	76
138	2/21/2014	LC 28C	10	-	< 1590	5	256	257
139	2/21/2014	LC 28C	10	-	< 1590	5	243	244
140	2/21/2014	LC 28T	10	205	400	5	265	139
141	2/21/2014	LC 28T	10	205	400	5	264	140
142	2/21/2014	LC 29C	5	-	< 1590	5	128	128
143	2/21/2014	LC 29C	5	-	< 1590	5	123	125
144	2/21/2014	LC 29T	5	109	208	5	137	73
145	2/21/2014	LC 29T	5	109	208	5	135	75
* In-Line load cell LTT07 disconnected from clevis rod end. Hydraulic system dumped.								

8.2.11 Test Data Summary

A summary of the buckling loads for all of the test articles is presented in table 12. For compression test runs, the average jack load for each load case is shown. For torsion test runs, the average upper jack load, the average lower jack load, and their difference are shown. As for the buckling load trends, the lower the test article pressure the lower the buckling load. Also, the smaller the test article the more applied load was required to reach buckling.

Table 12. Test data summary.

Test Article	COMPRESSION				TORSION											
	Average Jack Load (Lbf)				Average Upper Jack Load (Lbf)				Average Lower Jack Load (Lbf)				Torsional Load - Difference Between Upper and Lower Jack Loads (Lbf)			
	20 PSI	15 PSI	10 PSI	5 PSI	20 PSI	15 PSI	10 PSI	5 PSI	20 PSI	15 PSI	10 PSI	5 PSI	20 PSI	15 PSI	10 PSI	5 PSI
T5C-1	237	177	113	**	244	181	117	**	136	104	65	**	108	77	52	
T5A-1	455	314	261	192	660	*	383	208	10	*	88	92	650		295	116
T5B-1	226	209	**	**	**	**	**	**	**	**	**	**				
T5B-2	352	301	250	126	516	402	265	136	42	72	140	74	474	330	125	62
T4A-1	494	411	345	188	803	*	398	195	209	*	99	93	594		299	103
T4A-2	449	380	287	189	723	572	385	197	100	91	53	90	623	481	332	107
T4A-3	**	395	302	190	**	569	383	207	**	65	86	94		504	297	113
T3A-4	702	568	384	187	802	600	387	193	167	248	200	98	635	352	187	95
Notes:	* Did not buckle ** Did not test															

8.3 Observations

The multiple types of instrumentation in place allowed test engineers to monitor both the test article responses and the effectiveness of the test hardware. There were several findings related to these, based on the review of test data.

8.3.1 Buckling Event

The buckling events were the main focus of the testing. Observations made both from instrumentation data and from visual observations are discussed in the following sections.

8.3.1.1 Buckling Detection - During buckling events, the test articles deformed significantly; buckling could be detected simply by visual observations. The buckling loads, however, or the exact loads at which the structural instability began, were not as easy to discern. For the purpose of comparing test article buckling loads between test runs during testing, a simple and quick method was used to identify the approximate buckling loads. In-depth research on the structural characteristics of the test article, however, may require a more sophisticated method to obtain more accurate buckling loads. The following sections describe the simplified method used during testing, and present other observations that were made during the buckling events.

8.3.1.2 Horizontal String Pots - The primary method used to obtain the approximate buckling loads was to observe changes of the average horizontal string pot curve. In one IADS® display, the time history plots of the average upper hydraulic jack loads, the average lower hydraulic jack loads, and the average horizontal string pots values were displayed together as shown in the IADS® screenshot presented as figure 41.

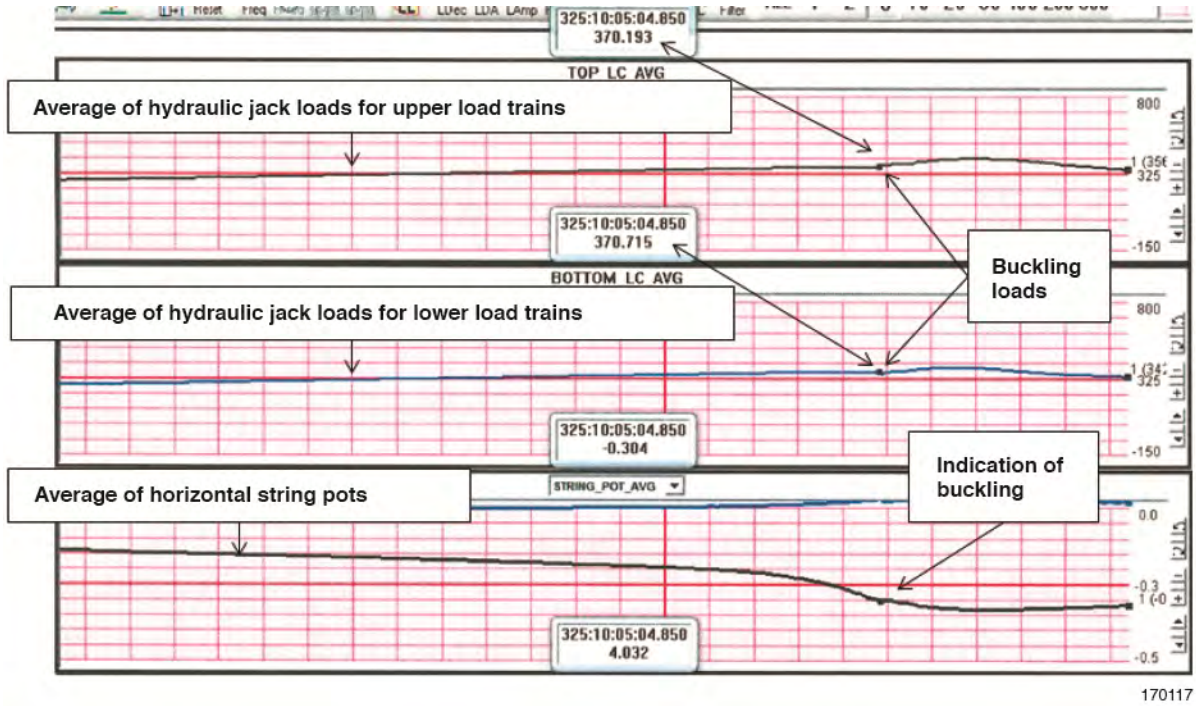

Figure 41. Buckling event as shown in the real-time horizontal string potentiometer data (test run #69 / T4A-2 / 15 psi / compression).

The lower plot contains a dot identified by an arrow and the label “Indication of Buckling” placed where the curve had a sudden slope change. At approximately the same time, the curves for the jack loads (middle and upper plots) can be seen to have had slope changes. For this test, the buckling loads were determined to be 370 lbf and 371 lbf for the upper and lower hydraulic jacks, respectively.

8.3.1.3 Liquid Metal Strain Gage - The real-time LMSG time history plots also served very well as buckling indicators. Figure 42 shows the same buckling event as that described in the previous section. In this figure, the red vertical dashed line represents the time at which buckling onset was assumed according to the horizontal string pot data described in the previous section. As can be seen in figure 42, majority of the LMSG curves changed slopes at this moment as well.

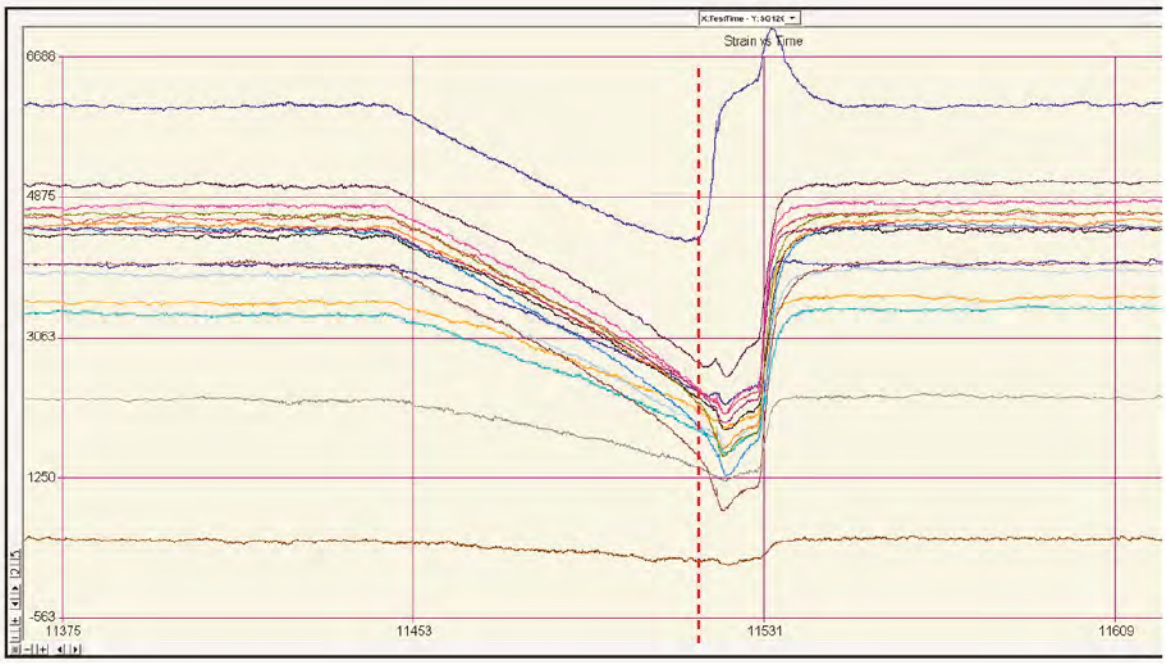

Figure 42. Buckling event as shown in the real-time liquid metal strain gage time history plot (test run #69 / T4A-2 / 15 psi / compression).

8.3.1.4 Hydraulic Jack Load Cell Feedback - The MLCS was programmed to compare the loads that were commanded to the hydraulic jacks against the feedback loads that were measured by the load cells. If any of the differences between the commanded and the measured loads were greater than the pre-programmed value of 40 lbf, then the MLCS automatically changed the control mode to hold the actuators at their current positions.

During loading, the control software adjusted the servovalve current (which regulated the pressure to the actuator to control the applied force) in an ongoing attempt to match the commanded loads. As the test article was loaded, forces were evenly applied by the MLCS and evenly resisted by the test article. As the test article buckled, the resistance force collapsed in certain regions and could cause the difference between the commanded and the measured loads to exceed 40 lbf.

During testing, there were several instances in which the MLCS automatically went into control mode, which provided another confirmation of the occurrence of the buckling of the test article.

8.3.1.5 Visual Observation - The buckled shape of the test articles were either in-plane or out-of-plane. During out-of-plane buckling, the test article could deflect several inches vertically in both directions, as shown in figure 43. In this case, test article buckling was easily detected by visual observation.

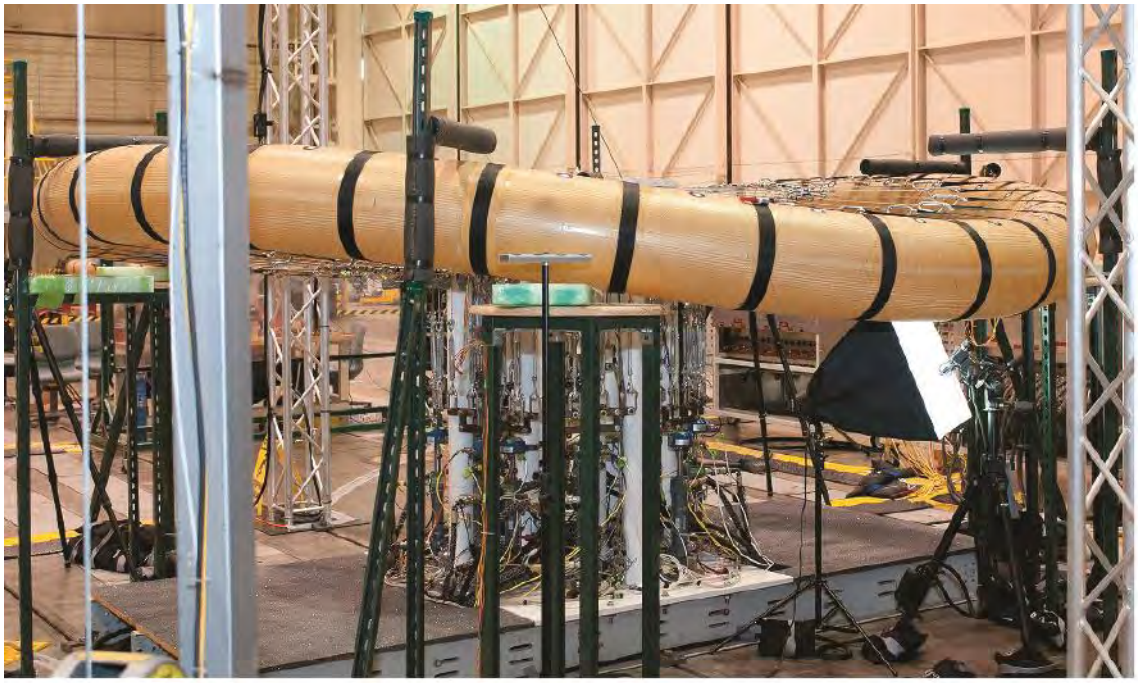

170119

Figure 43. Out-of-plane buckling (test run #1 / T5C-1 / 20 psi / compression).

In-plane buckling was not as easy to detect visually, because test personnel on the FLL floor observed the test article from approximately the same horizontal plane. Figure 44 shows a typical in-plane buckle as indicated by the "flat" region of the test article in the right-hand image.

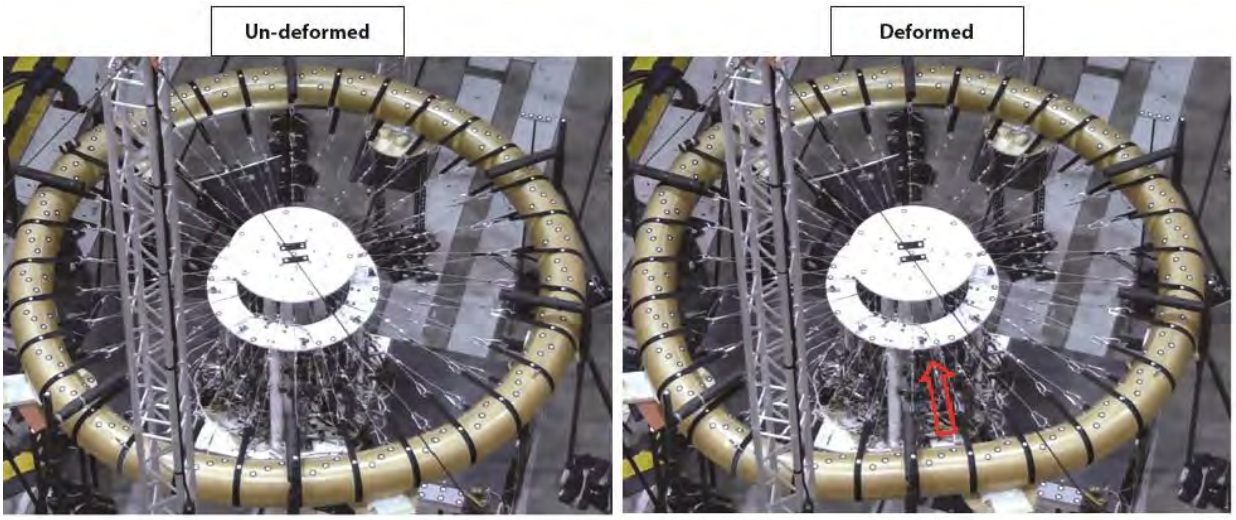

170120

Figure 44. In-plane buckling (test run #22 / T5A-1 / 20 psi / compression).

8.3.1.6 ARAMIS Strain Measurement System - The ARAMIS system provided strain images of a particular area on the test article, showing how the applied loads and some of the features on the test article affected the strain levels. Figure 45 shows strain images of the un-deformed (no-load) and the deformed (buckled) states of the test article. The right-hand buckled image shows negative strains, as the test article

was being pulled and deformed toward its center. The dark blue lines in the right-hand image seem to reflect the braid directions.

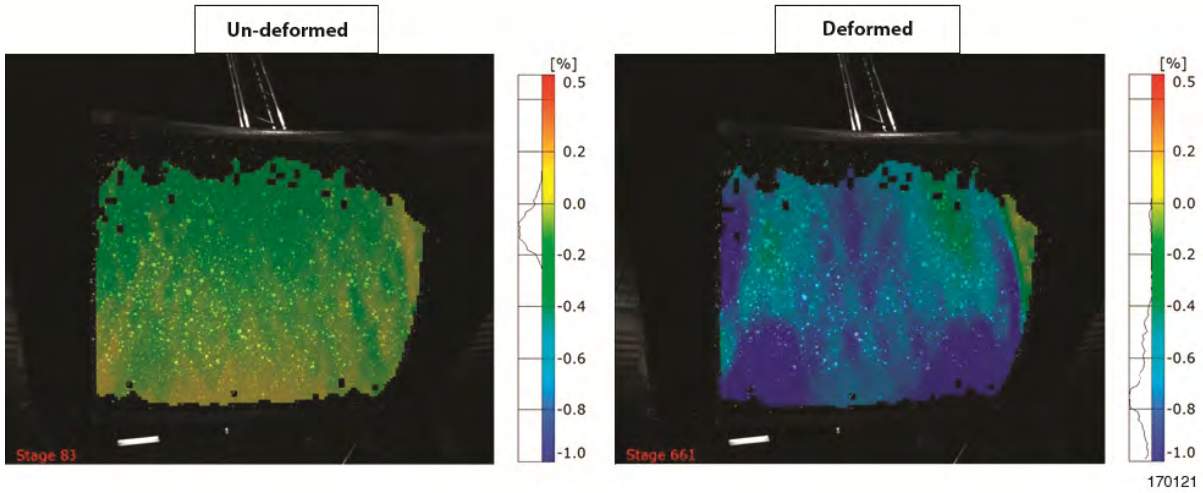

Figure 45. ARAMIS strain images of no-load (left) and loaded and buckled (right) (test run #45 / T4A-3 / 15psi / compression).

In this test run, the buckled shape was in-plane and the area of the ARAMIS pattern had little global displacement, so the buckled image was still centered in the camera field of view. In some out-of-plane buckling events, however, the vertical displacements of the test article were so great that the ARAMIS pattern partially moved outside of the camera field of view and only partial strain images were obtained.

8.3.1.7 PONTOS Displacement Measurement System - Although not available in real time, the PONTOS data captured during buckling provided a set of more detailed displacement data compared to the string-pot data. The PONTOS system captured the spatial displacement data of roughly 100 targets that were placed on the test article. Figure 46 shows target displacements in the Y direction.

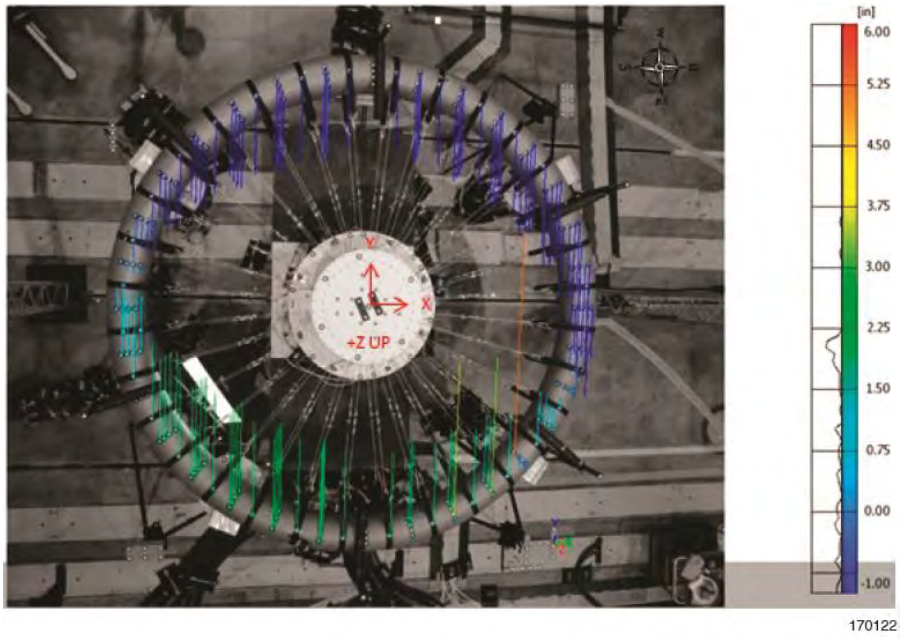

Figure 46. PONTOS Y-displacement vectors (test run #1 / T5C-1 / 20 psi / compression).

8.3.2 Pulley Friction Loss

The load applied onto the test article originated from the hydraulic jacks. In order for each hydraulic jack load to reach the test article, however, it had to travel through several hardware components in the load train. One of the critical parts in the load train was the pulley, which allowed the applied load to change direction from vertical to horizontal. The disadvantage of using a pulley in the load train is that it slightly reduces the applied load due to internal friction. Figure 47 shows the compression load profile from test run number 30 as measured by the sum of all 16 hydraulic jack load cells (black) and by the sum of all 64 in-line load cells (red). Each curve shows the total loads measured by each type of instrumentation. The load reduction caused by pulley friction is very noticeable as indicated by the difference between the two curves in the figure. At peak load, there was approximately a 6% reduction in load actually applied to the test article.

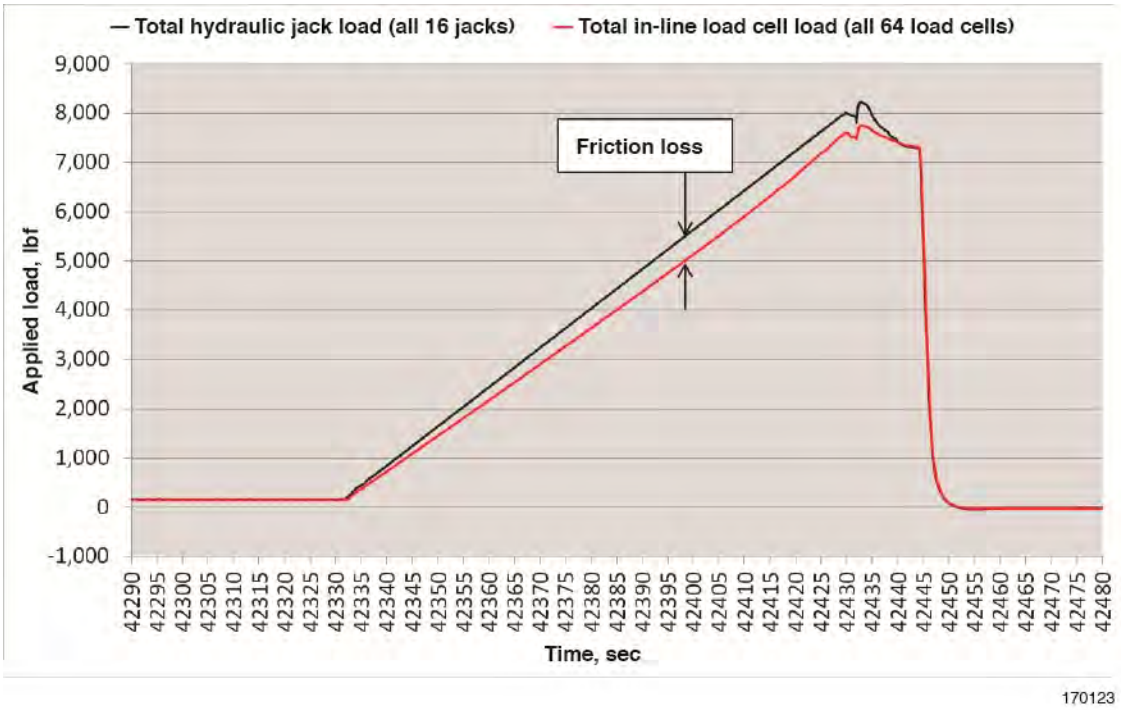

Figure 47. Total applied loads measured by the sum of the 16 hydraulic jack load cells (black line) and by the sum of the 64 in-line load cells (red line) (test run #30 / T4A-1 / 20 psi / compression).

Another way of evaluating the magnitude of the friction loss is to consider the differences in loads between a hydraulic jack load cell (the black line in figure 48) and the total load of its four associated in-line load cells (the red line in figure 48). Figure 48 shows that the friction loss is significant. For the presented case there was an approximately 9% reduction in applied load.

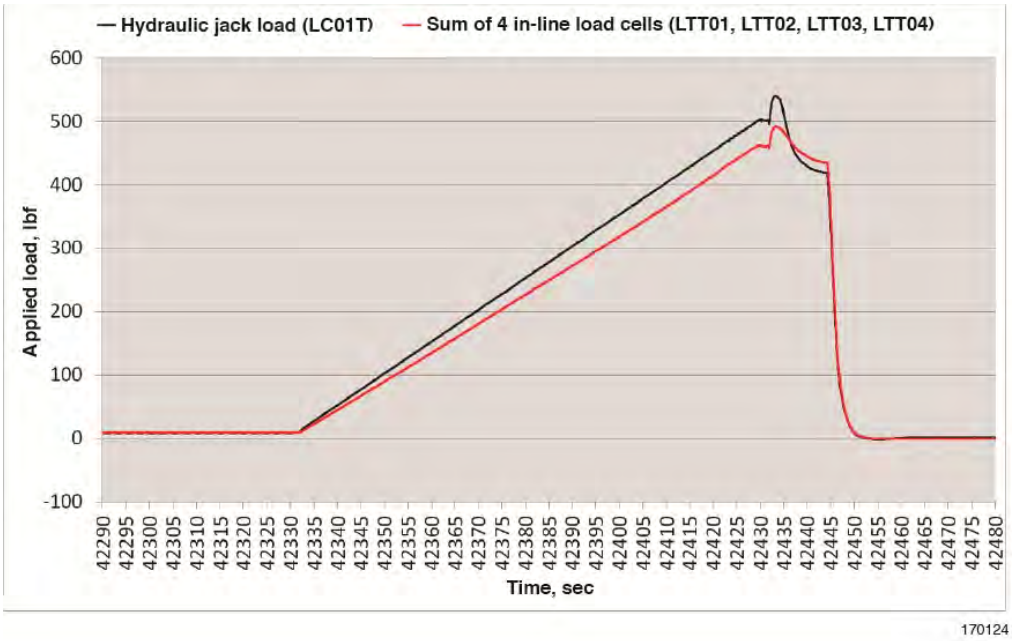

Figure 48. Applied loads measured by hydraulic jack T01 (black line) and the sum of 4 in-line load cells (red line) in the same load train (test run #30 / T4A-1 / 20 psi / compression).

One of the effects of the pulley friction loss on the testing was that the friction coefficients for the pulleys were not exactly the same, so loads were not evenly applied to the test article. Figure 49 shows that the four in-line load cell loads from the same whiffletree system had different loads.

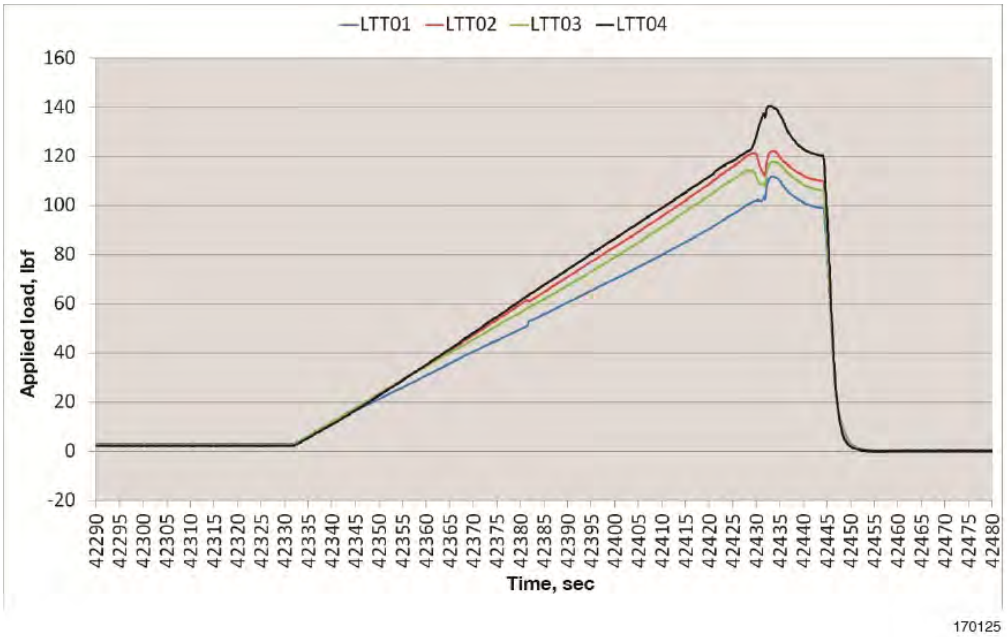

Figure 49. Applied loads measured by the four in-line load cells in load train T01 (test run #30 / T4A-1 / 20 psi / compression).

8.3.3 Benefits of Pre-Test Pressure Cycles

Hysteresis in LMSG data was noticed during the test setup checkout operation while the test article was being inflated and deflated. The test article appeared to require a few pressure cycles to condition it to reduce the hysteresis. It was further observed that the number of pressure cycles needed could be as many as three. The checklist thus was modified so that on each test day, up to three pressure cycles would be performed until the hysteresis observed in the LMSG data was within 500 micro-strain. The checklist also specified to zero the LMSG data after each pressure cycle. Figure 50 shows three pressure cycles performed on the T4A-1 test article. It can be seen that the hysteresis reduced as the test article went through each pressure cycle. The hysteresis was very significant after the first cycle, however, it was nearly nonexistent by the end of the third cycle.

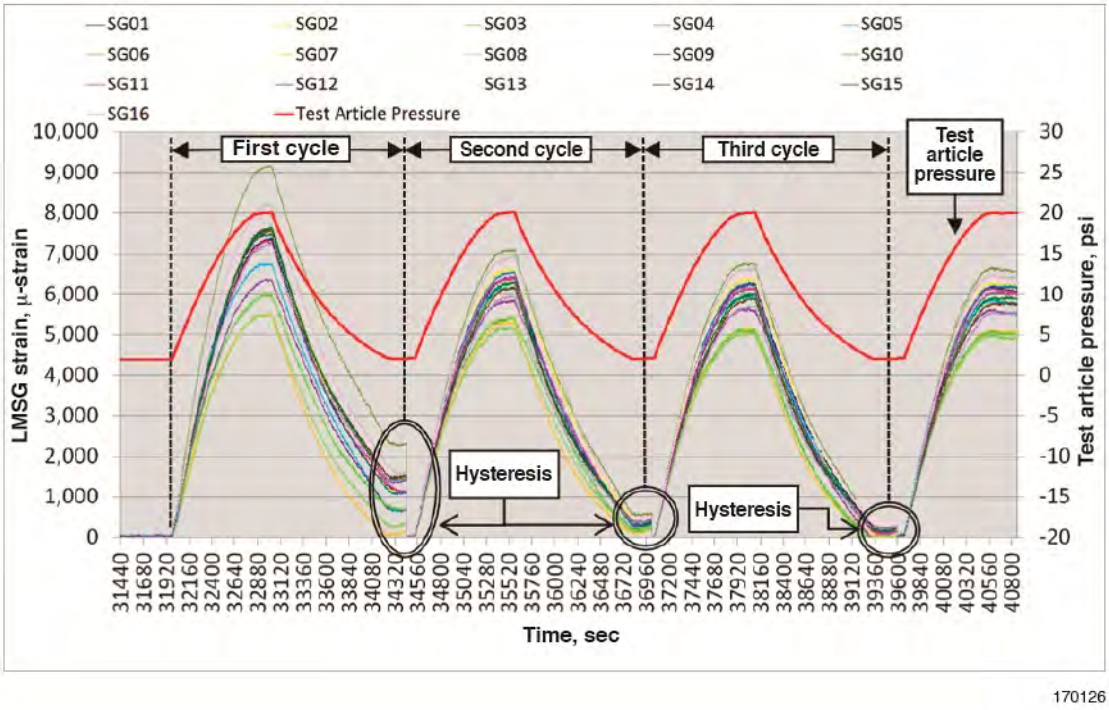

Figure 50. Pressure cycles and hysteresis reductions (prior to test run #26 / T4A-1).

8.3.4 Conditions That Affected Test Article Pressure

Once the test article was inflated to the test pressure, the flow valve on the test article inflation and deflation port was closed and the air supply line to the test article was disconnected. Although the test article pressure was not controlled during loading, it was always monitored and recorded.

8.3.4.1 Change Due to Applied Loads - Figure 51 shows pressure change during a compression test run. In this case, the test article pressure (black line) increased as the mechanical loads (blue line and red line) were applied. As observed in the figure, this increase vanished after the test article buckled and the applied loads were removed.

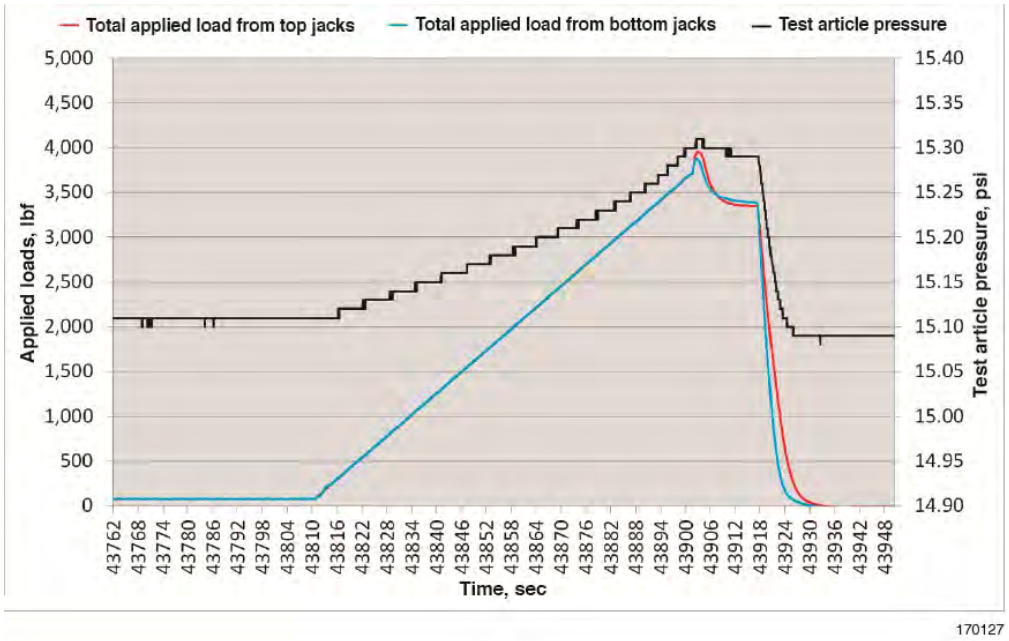

Figure 51. Test article pressure response during compression loading (test run #45 / T4A-3 / 15 psi / compression).

Likewise for torsion cases, the applied loads affected the test article pressure. As shown in figure 52, the test article pressure (black line) increased as the load profiles (blue line and red line) increased to the ramp-up load. As the applied loads remained constant during the ramp-up hold, the pressure remained constant as well. When the applied loads continued to the target loads for the upper and lower straps, the test article pressure increased, even though the net applied load remained constant. This increase in pressure most likely was due to the slow deformation of the torus cross-section.

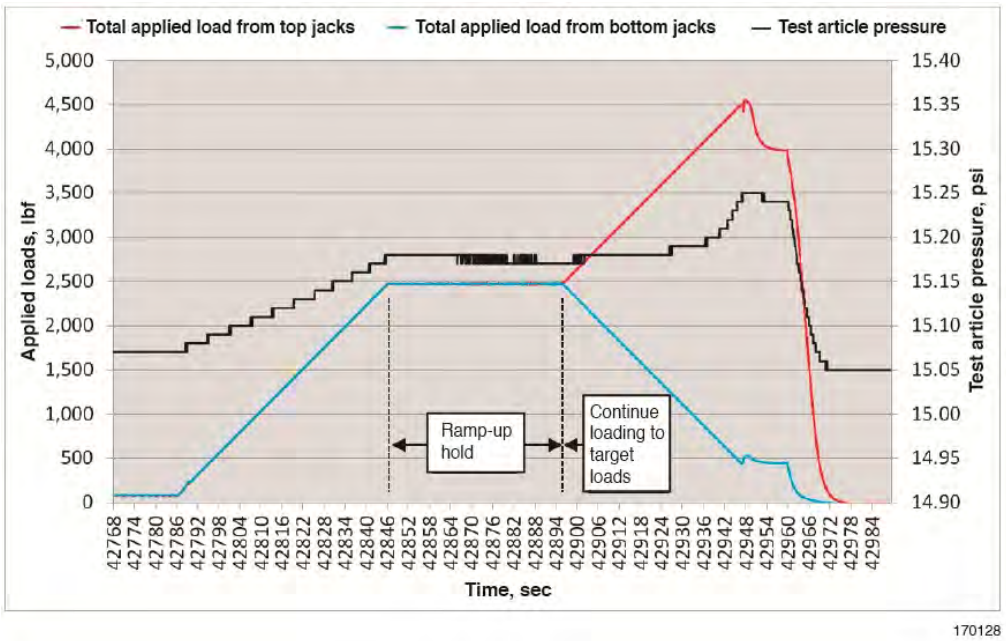

Figure 52. Test article pressure response during torsion loading (test run #49 / T4A-3 / 15 psi / torsion).

8.3.4.2 Change Due to Test Area Temperature - The checklist required the test article pressure to be within 0.1 psi of the test pressure at the time when loading began. If the test article pressure fluctuated outside of this tolerance, inflation or deflation had to be performed to bring the pressure to within the required range. Figure 53 shows that the temperature-pressure relationship is fundamental and expected. In a time frame of 1.5 hr between tests, the test area temperature (red line) increased by approximately 1.5 °F while the test article pressure (black line) responded with a 0.13-psi increase.

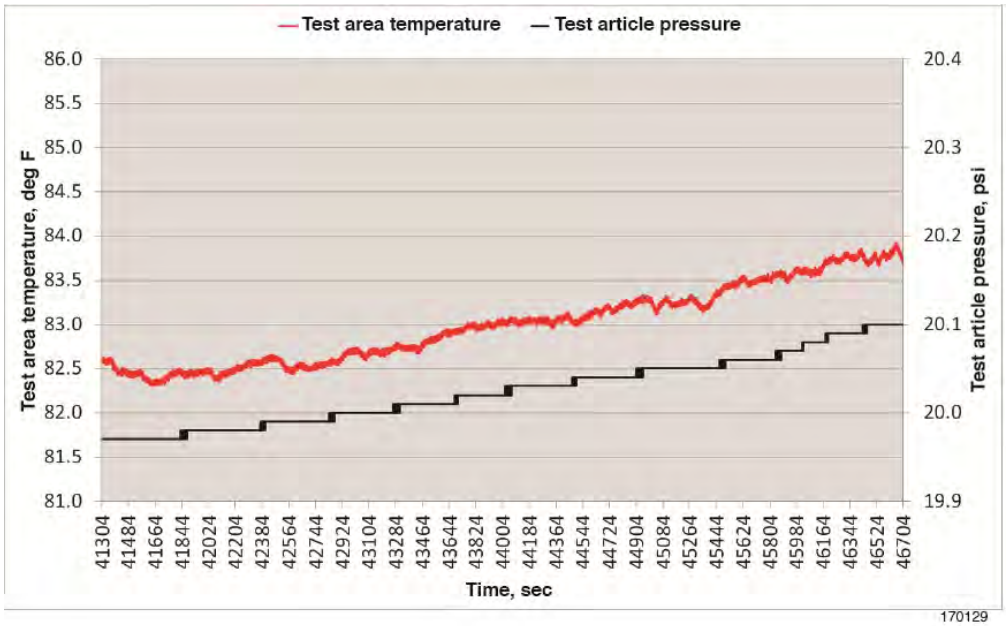

Figure 53. Test article pressure varies with test area temperature.

During the same time frame, the average LMSG value (black line) or the cord strains also increased (figure 54), which is in agreement with the pressure increase.

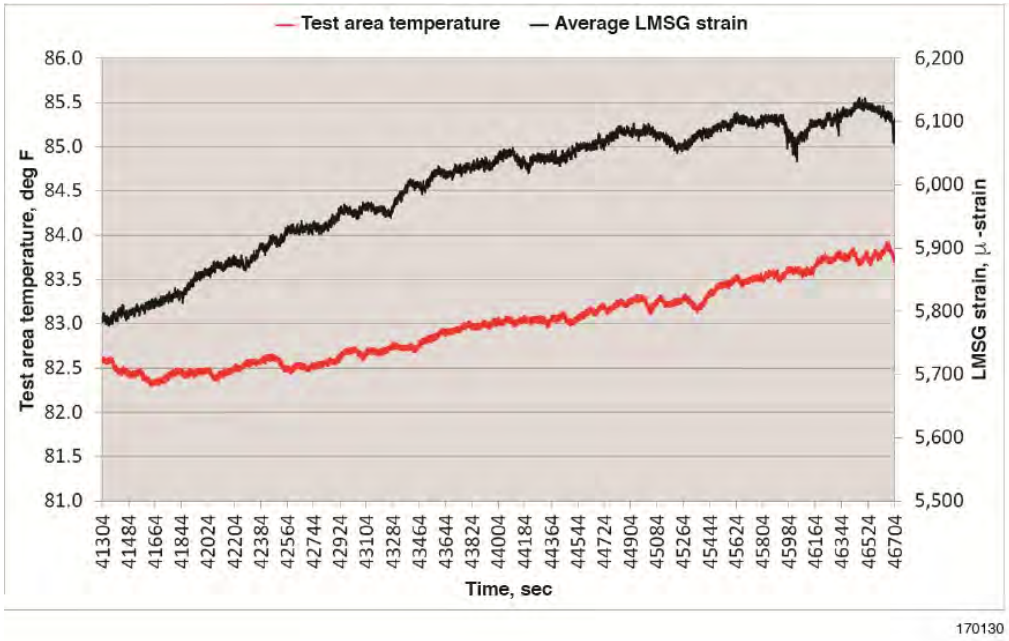

Figure 54. Average LMSG value varies with test area temperature.

8.4 Anomalies During Testing

Although anomalies can cause schedule delays, recovering from anomalies usually increases the awareness of similar potential issues and helps the test team to become more efficient and effective. The following sections describe some of the issues encountered during HIAD testing.

8.4.1 Jack Stroke Limitations

The available hydraulic jack stroke was 6 in for most of the jacks. This stroke was assumed to be more than sufficient to accommodate the largest test article deformation prior to buckling despite the use of turnbuckles to maximize the available jack stroke for each load case. Instances arose, however, when the hydraulic jacks ran out of stroke prior to the buckling of the test article. Extra stroke likely was needed because, contrary to the assumption made during the design of the test setup, the deformation of the test article was not uniform. See figure 44 depicting an in-plane buckling event, especially the section of the test article where the red arrow is deformed inward toward the center while some other sections are deformed outward. This non-circular and non-uniform deformation caused the test article to experience larger-than-expected local displacement prior to buckling.

8.4.2 Load Train Disconnected During Testing

Due to the frequent turnbuckle adjustments required to maximize the available jack stroke for loading, the load train cable connection became loose and eventually disconnected during the loading of test article T5B-2 during test run number 127. Once pre-load had been applied, turnbuckles, as needed, were adjusted to maximize the jack travel in the direction of loading. It is very likely that turning the turnbuckle body (figure 55) also rotated the cable that routed through the pulley. It is believed that this rotation unscrewed the threaded connection between the clevis rod end and the in-line load cell (figure 56).

Figure 55. Turnbuckle adjustments were made to provide more available jack stroke.

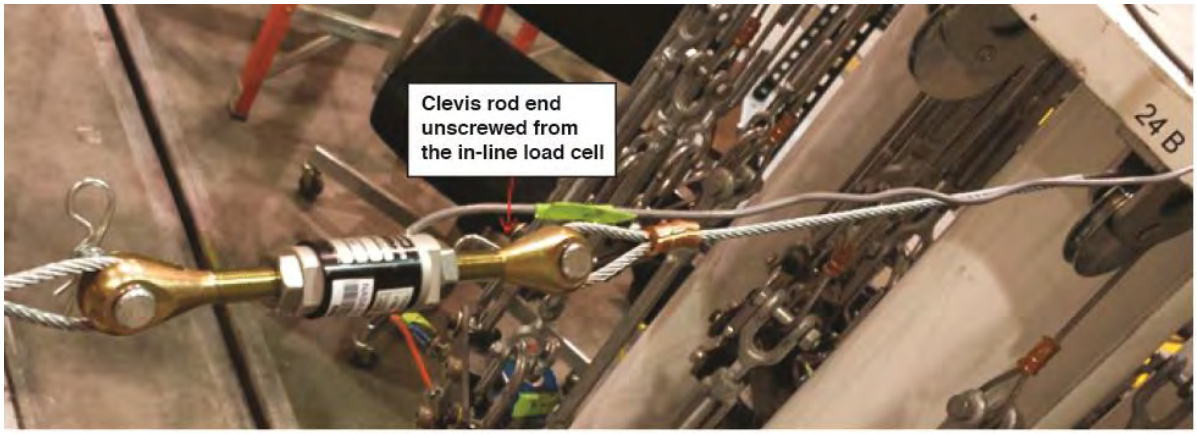

170132

Figure 56. Clevis rod end connection to in-line load cell.

During test run number 127, the clevis rod end disconnected from in-line load cell LTT17 during loading. Figure 57 shows that at approximately 46,084 seconds, the load on LTT17 (red line) jumped back down to zero. The MLCS detected this large difference between the commanded load and the feedback load, which difference exceeded the pre-programmed failsafe value set in the MLCS software. The MCLS thus properly initiated an automatic dump of the hydraulic pump, removing all hydraulic jack loads (black line in figure 57). Subsequent load train inspection indicated that a few other connections between a clevis rod end and its in-line load cell were loose. The test team was then advised to avoid rotating the cables and to periodically check the threaded connections on the in-line load cells. This event also showed that the safety feature in the MLCS worked properly and prevented damage to the test article or the test setup hardware.

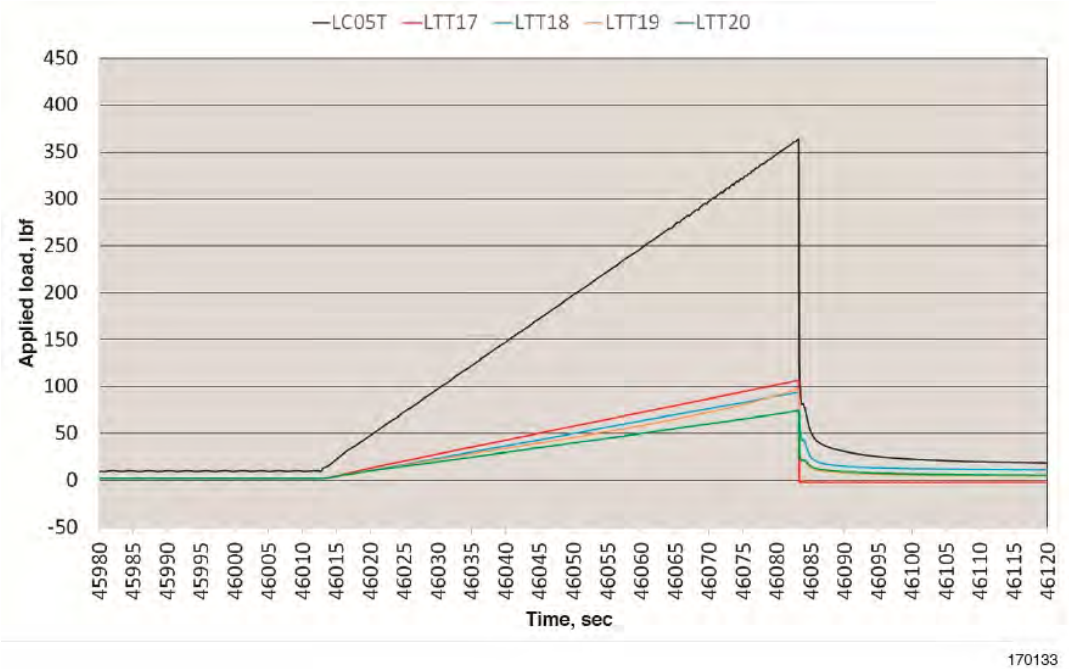

170133

Figure 57. Load cell output during separation of in-line load cell in clevis rod end (test run #127 / T5B-2 / 20 psi / compression).

9.0 Summary

The National Aeronautics and Space Administration (NASA) Armstrong Flight Research Center Flight Loads Laboratory test team was tasked by the NASA Langley Research Center (LaRC) with load-testing the eight Hypersonic Inflatable Aerodynamic Decelerator (HIAD) test articles in order to obtain displacement and strain data. Testing was successful, as all but a few test runs resulted in the buckling of the test article. The required test data for applied load, strain, displacement, and photogrammetry were obtained and sent to LaRC to help with the validation and construction of the finite element model of the HIAD assembly.

Appendix A: Test Matrix

Table A-1. Test matrix (1 of 2).

Test Article	Load Case	Pressure	Loading Type	Predicted Buckling Load		Maximum Applied Load (per Strap-End)
				Upper Strap-End	Lower Strap-End	
		(psi)		(lbf)	(lbf)	(lbf)
T5C-1	LC 1C	20	Compression	80-100	80-100	400
	LC 1T		Torsion	86	43	86
	LC 2C	15	Compression	60-80	60-80	400
	LC 2T		Torsion	60	30	60
	LC 3C	10	Compression	40-60	40-60	400
	LC 3T		Torsion	40	20	40
	LC 4C	5	Compression	20-40	20-40	400
	LC 4T		Torsion	20	10	20
T5A-1	LC 5C	20	Compression	200-250	200-250	400
	LC 5T		Torsion	200	100	200
	LC 6C	15	Compression	150-200	150-200	400
	LC 6T		Torsion	150	75	150
	LC 7C	10	Compression	100-150	100-150	400
	LC 7T		Torsion	100	50	100
	LC 8C	5	Compression	50-100	50-100	400
	LC 8T		Torsion	54	27	54
T4A-1	LC 9C	20	Compression	200-250	200-250	400
	LC 9T		Torsion	200	100	200
	LC 10C	15	Compression	150-200	150-200	400
	LC 10T		Torsion	150	75	150
	LC 11C	10	Compression	100-150	100-150	400
	LC 11T		Torsion	100	50	100
	LC 12C	5	Compression	50-100	50-100	400
	LC 12T		Torsion	54	27	54
T4A-2	LC 13T	20	Torsion	200	100	200
	LC 13C		Compression	200-250	200-250	400
	LC 14T	15	Torsion	150	75	150
	LC 14C		Compression	150-200	150-200	400
	LC 15T	10	Torsion	100	50	100
	LC 15C		Compression	100-150	100-150	400
	LC 16T	5	Torsion	54	27	54
	LC 16C		Compression	50-100	50-100	400

Table A-2. Test matrix (2 of 2).

Test Article	Load Case	Pressure	Loading Type	Predicted Buckling Load		Maximum Applied Load (per Strap-End)
				Upper Strap-End	Lower Strap-End	
		(psi)		(lbf)	(lbf)	(lbf)
T4A-3	LC 17C	15	Compression	150-200	150-200	400
	LC 17T		Torsion	160	80	160
	LC 18C	10	Compression	100-150	100-150	400
	LC 18T		Torsion	110	55	110
	LC 19C	5	Compression	50-100	50-100	400
	LC 19T		Torsion	59	30	59
T3A-4	LC 20C	20	Compression	200-250	200-250	400
	LC 20T		Torsion	200	100	200
	LC 21C	15	Compression	150-200	150-200	400
	LC 21T		Torsion	150	75	150
	LC 22C	10	Compression	100-150	100-150	400
	LC 22T		Torsion	100	50	100
	LC 23C	5	Compression	50-100	50-100	400
	LC 23T		Torsion	54	27	54
T5B-1*	LC 24C	20	Compression	<400	<400	400
	LC 24T		Torsion	N/A**	N/A**	N/A**
	LC 25C	15	Compression	<400	<400	400
	LC 25T		Torsion	N/A**	N/A**	N/A**
	N/A	10	Compression	<400	<400	400
	N/A		Torsion	N/A**	N/A**	N/A**
	N/A	5	Compression	<400	<400	400
	N/A		Torsion	N/A**	N/A**	N/A**
T5B-2*	LC 26C	20	Compression	<400	<400	400
	LC 26T		Torsion	N/A**	N/A**	N/A**
	LC 27C	15	Compression	<400	<400	400
	LC 27T		Torsion	N/A**	N/A**	N/A**
	LC 28C	10	Compression	<400	<400	400
	LC 28T		Torsion	N/A**	N/A**	N/A**
	LC 29C	5	Compression	<400	<400	400
	LC 29T		Torsion	N/A**	N/A**	N/A**

* Added to Test Matrix near the end of the original test program

** Prediction not provided. However load profile can be calculated based on Compression results.

Appendix B: Braid Angle Measurement

Braid angle measurement was performed by measuring the horizontal distance between tracer thread crossings by using a tape measure. As shown by the green lines in figure B-1, the distance was measured from point 1 to point 2, then from point 2 to point 3 and so on. This was done around the whole circumference. The average of these horizontal distances was considered as the run value. Another measurement taken was the tube perimeter at each tracer thread crossing. The average value of this measurement was considered as the rise value. The red line in the figure further illustrates that the tracer line travels two horizontal distances as it makes one revolution around the tube. Therefore, the braid angle, θ, was calculated as shown in equation (B-1):

$$\theta = \tan^{-1} \frac{\text{RISE}}{2 \times \text{RUN}} \tag{B-1}$$

where RISE is average value of the tube perimeters measured at tracer thread crossings, and RUN is the average value of the horizontal distances between adjacent tracer thread crossings.

This process was performed for both the inner and outer radius of the test article.

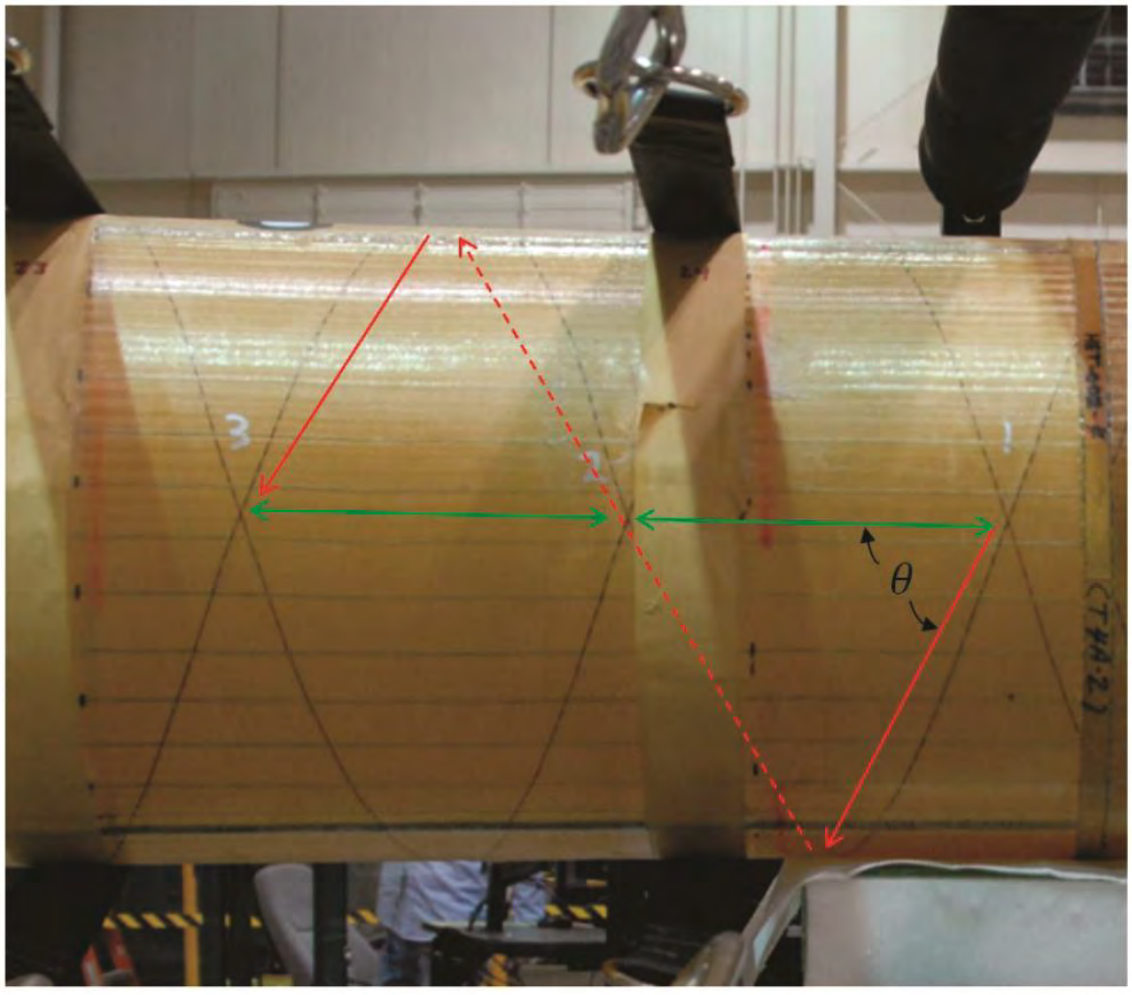

Figure B-1. Braid angle measurement.

The results of the measured braid angles are shown in Table B-1. The small differences indicated that the test articles had negligible braid angle changes before and after test.

Table B-1. Braid angle measurement results.

Test Article	Measured Braid Angle (deg)			
	Pre-Test		Post-Test	
	Inner Radius	Outer Radius	Inner Radius	Outer Radius
T4A-1	71.6	68.0	71.6	68.0
T4A-3	71.2	67.5	71.1	67.4
T4A-2	71.5	67.9	71.5	67.8
T3A-4	71.8	67.5	71.7	67.4
T5A-1*	71.5	68.4	71.5	68.4
T5B-1	65.8	62.1	65.8	62.0
T5B-2	66.2	62.5	66.2	62.4
* Measurement done for Feb 2014 re-test.				

Appendix C: Data Acquisition System Instrumentation Channel List

Information on instrumentation recorded by the data acquisition system is shown in Table C-1, Table C-2, and Table C-3.

Table C-1. Data acquisition system channel list (1 of 3).

	Channel Name	Type of Channel	Excitation (volts)	Engineering Units (EU)	Range of Tranducer	Transducer Precision	Location
1	SG01	Liquid Gage	15	mV	+\-.1 Volts	Developmental Instrumentation 5% of Full Scale	at strap 9, upper cord
2	SG02	Liquid Gage	15	mV	+\-.1 Volts		at strap 9, lower cord
3	SG03	Liquid Gage	15	mV	+\-.1 Volts		between straps 8 & 9, upper cord
4	SG04	Liquid Gage	15	mV	+\-.1 Volts		between straps 8 & 9, lower cord
5	SG05	Liquid Gage	15	mV	+\-.1 Volts		at strap 29, upper cord
6	SG06	Liquid Gage	15	mV	+\-.1 Volts		at strap 29, lower cord
7	SG07	Liquid Gage	15	mV	+\-.1 Volts		between straps 28 & 29, upper cord
8	SG08	Liquid Gage	15	mV	+\-.1 Volts		between straps 28 & 29, lower cord
9	SG09	Liquid Gage	15	mV	+\-.1 Volts		at strap 21, upper cord
10	SG10	Liquid Gage	15	mV	+\-.1 Volts		at strap 21, lower cord
11	SG11	Liquid Gage	15	mV	+\-.1 Volts		between straps 20 & 21, upper cord
12	SG12	Liquid Gage	15	mV	+\-.1 Volts		between straps 20 & 21, lower cord
13	SG13	Liquid Gage	15	mV	+\-.1 Volts		between straps 13 & 14, upper cord mid point between straps
14	SG14	Liquid Gage	15	mV	+\-.1 Volts		between straps 13 & 14, lower cord closer to strap 14
15	SG15	Liquid Gage	15	mV	+\-.1 Volts		between straps 13 & 14, lower cord mid point between straps
16	SG16	Liquid Gage	15	mV	+\-.1 Volts		between straps 13 & 14, lower cord closer to strap 13
17	POT01	Linear	9.95	IN	6 in	0.1% of Full Scale	between straps 2 & 3
18	POT02	Linear	9.95	IN	6 in	0.1% of Full Scale	between straps 6 & 7
19	POT03	Linear	9.95	IN	6 in	0.1% of Full Scale	between straps 10 & 11
20	POT04	Linear	9.95	IN	6 in	0.1% of Full Scale	between straps 14 & 15
21	POT05	Linear	9.95	IN	6 in	0.1% of Full Scale	between straps 18 & 19
22	POT06	Linear	9.95	IN	6 in	0.1% of Full Scale	between straps 22 & 23
23	POT07	Linear	9.95	IN	6 in	0.1% of Full Scale	between straps 26 & 27
24	POT08	Linear	9.95	IN	6 in	0.1% of Full Scale	between straps 30 & 31
25	POT09	Linear	9.95	IN	36 in	0.1% of Full Scale	vertical displacement btw straps 2 & 3
26	POT10	Linear	9.95	IN	36 in	0.1% of Full Scale	vertical displacement btw straps 6 & 7
27	POT11	Linear	9.95	IN	42 in	0.1% of Full Scale	vertical displacement btw straps 10 & 11
28	POT12	Linear	9.95	IN	42 in	0.1% of Full Scale	vertical displacement btw straps 14 & 15
29	POT13	Linear	9.95	IN	36 in	0.1% of Full Scale	vertical displacement btw straps 18 & 19
30	POT14	Linear	9.95	IN	36 in	0.1% of Full Scale	vertical displacement btw straps 22 & 23
31	POT15	Linear	9.95	IN	30 in	0.1% of Full Scale	vertical displacement btw straps 26 & 27
32	POT16	Linear	9.95	IN	24 in	0.1% of Full Scale	vertical displacement btw straps 30 & 31
33	LC01T	Load Cell	9.95	LBS	2000	0.02% of Full Scale	connects to straps 1,2,3,4 for top load train
34	LC02T	Load Cell	9.95	LBS	2000	0.02% of Full Scale	connects to straps 5,6,7,8 for top load train
35	LC03T	Load Cell	9.95	LBS	2000	0.02% of Full Scale	connects to straps 9,10,11,12 for top load train
36	LC04T	Load Cell	9.95	LBS	2000	0.02% of Full Scale	connects to straps 13,14,15,16 for top load train
37	LC05T	Load Cell	9.95	LBS	2000	0.02% of Full Scale	connects to straps 17,18,19,20 for top load train
38	LC06T	Load Cell	9.95	LBS	2000	0.02% of Full Scale	connects to straps 21,22,23,24 for top load train
39	LC07T	Load Cell	9.95	LBS	2000	0.02% of Full Scale	connects to straps 25,26,27,28 for top load train
40	LC08T	Load Cell	9.95	LBS	2000	0.02% of Full Scale	connects to straps 29,30,31,32 for top load train

Table C-2. Data acquisition system channel list (2 of 3).

	Channel Name	Type of Channel	Excitation (volts)	Engineering Units (EU)	Range of Tranducer	Transducer Precision	Location
41	LC01B	Load Cell	9.95	LBS	2000	0.02% of Full Scale	connects to straps 1,2,3,4 for bottom load train
42	LC02B	Load Cell	9.95	LBS	2000	0.02% of Full Scale	connects to straps 5,6,7,8 for bottom load train
43	LC03B	Load Cell	9.95	LBS	2000	0.02% of Full Scale	connects to straps 9,10,11,12 for bottom load train
44	LC04B	Load Cell	9.95	LBS	2000	0.02% of Full Scale	connects to straps 13,14,15,16 for bottom load train
45	LC05B	Load Cell	9.95	LBS	2000	0.02% of Full Scale	connects to straps 17,18,19,20 for bottom load train
46	LC06B	Load Cell	9.95	LBS	2000	0.02% of Full Scale	connects to straps 21,22,23,24 for bottom load train
47	LC07B	Load Cell	9.95	LBS	2000	0.02% of Full Scale	connects to straps 25,26,27,28 for bottom load train
48	LC08B	Load Cell	9.95	LBS	2000	0.02% of Full Scale	connects to straps 29,30,31,32 for bottom load train
49	LTT01	Load Cell	9.95	LBS	1000	0.6% of Full Scale	strap 1, top load train
50	LTT02	Load Cell	9.95	LBS	1000	0.6% of Full Scale	strap 2, top load train
51	LTT03	Load Cell	9.95	LBS	1000	0.6% of Full Scale	strap 3, top load train
52	LTT04	Load Cell	9.95	LBS	1000	0.6% of Full Scale	strap 4, top load train
53	LTT05	Load Cell	9.95	LBS	1000	0.6% of Full Scale	strap 5, top load train
54	LTT06	Load Cell	9.95	LBS	1000	0.6% of Full Scale	strap 6, top load train
55	LTT07	Load Cell	9.95	LBS	1000	0.6% of Full Scale	strap 7, top load train
56	LTT08	Load Cell	9.95	LBS	1000	0.6% of Full Scale	strap 8, top load train
57	LTT09	Load Cell	9.95	LBS	1000	0.6% of Full Scale	strap 9, top load train
58	LTT10	Load Cell	9.95	LBS	1000	0.6% of Full Scale	strap 10, top load train
59	LTT11	Load Cell	9.95	LBS	1000	0.6% of Full Scale	strap 11, top load train
60	LTT12	Load Cell	9.95	LBS	1000	0.6% of Full Scale	strap 12, top load train
61	LTT13	Load Cell	9.95	LBS	1000	0.6% of Full Scale	strap 13, top load train
62	LTT14	Load Cell	9.95	LBS	1000	0.6% of Full Scale	strap 14, top load train
63	LTT15	Load Cell	9.95	LBS	1000	0.6% of Full Scale	strap 15, top load train
64	LTT16	Load Cell	9.95	LBS	1000	0.6% of Full Scale	strap 16, top load train
65	LTT17	Load Cell	9.95	LBS	1000	0.6% of Full Scale	strap 17, top load train
66	LTT18	Load Cell	9.95	LBS	1000	0.6% of Full Scale	strap 18, top load train
67	LTT19	Load Cell	9.95	LBS	1000	0.6% of Full Scale	strap 19, top load train
68	LTT20	Load Cell	9.95	LBS	1000	0.6% of Full Scale	strap 20, top load train
69	LTT21	Load Cell	9.95	LBS	1000	0.6% of Full Scale	strap 21, top load train
70	LTT22	Load Cell	9.95	LBS	1000	0.6% of Full Scale	strap 22, top load train
71	LTT23	Load Cell	9.95	LBS	1000	0.6% of Full Scale	strap 23, top load train
72	LTT24	Load Cell	9.95	LBS	1000	0.6% of Full Scale	strap 24, top load train
73	LTT25	Load Cell	9.95	LBS	1000	0.6% of Full Scale	strap 25, top load train
74	LTT26	Load Cell	9.95	LBS	1000	0.6% of Full Scale	strap 26, top load train
75	LTT27	Load Cell	9.95	LBS	1000	0.6% of Full Scale	strap 27, top load train
76	LTT28	Load Cell	9.95	LBS	1000	0.6% of Full Scale	strap 28, top load train
77	LTT29	Load Cell	9.95	LBS	1000	0.6% of Full Scale	strap 29, top load train
78	LTT30	Load Cell	9.95	LBS	1000	0.6% of Full Scale	strap 30, top load train
79	LTT31	Load Cell	9.95	LBS	1000	0.6% of Full Scale	strap 31, top load train
80	LTT32	Load Cell	9.95	LBS	1000	0.6% of Full Scale	strap 32, top load train
81	LTB01	Load Cell	9.95	LBS	1000	0.6% of Full Scale	strap 1, bottom load train
82	LTB02	Load Cell	9.95	LBS	1000	0.6% of Full Scale	strap 2, bottom load train
83	LTB03	Load Cell	9.95	LBS	1000	0.6% of Full Scale	strap 3, bottom load train
84	LTB04	Load Cell	9.95	LBS	1000	0.6% of Full Scale	strap 4, bottom load train
85	LTB05	Load Cell	9.95	LBS	1000	0.6% of Full Scale	strap 5, bottom load train
86	LTB06	Load Cell	9.95	LBS	1000	0.6% of Full Scale	strap 6, bottom load train
87	LTB07	Load Cell	9.95	LBS	1000	0.6% of Full Scale	strap 7, bottom load train
88	LTB08	Load Cell	9.95	LBS	1000	0.6% of Full Scale	strap 8, bottom load train
89	LTB09	Load Cell	9.95	LBS	1000	0.6% of Full Scale	strap 9, bottom load train
90	LTB10	Load Cell	9.95	LBS	1000	0.6% of Full Scale	strap 10, bottom load train
91	LTB11	Load Cell	9.95	LBS	1000	0.6% of Full Scale	strap 11, bottom load train
92	LTB12	Load Cell	9.95	LBS	1000	0.6% of Full Scale	strap 12, bottom load train
93	LTB13	Load Cell	9.95	LBS	1000	0.6% of Full Scale	strap 13, bottom load train

Table C-3. Data acquisition system channel list (3 of 3).

	Channel Name	Type of Channel	Excitation (volts)	Engineering Units (EU)	Range of Tranducer	Transducer Precision	Location
94	LTB14	Load Cell	9.95	LBS	1000	0.6% of Full Scale	strap 14, bottom load train
95	LTB15	Load Cell	9.95	LBS	1000	0.6% of Full Scale	strap 15, bottom load train
96	LTB16	Load Cell	9.95	LBS	1000	0.6% of Full Scale	strap 16, bottom load train
97	LTB17	Load Cell	9.95	LBS	1000	0.6% of Full Scale	strap 17, bottom load train
98	LTB18	Load Cell	9.95	LBS	1000	0.6% of Full Scale	strap 18, bottom load train
99	LTB19	Load Cell	9.95	LBS	1000	0.6% of Full Scale	strap 19, bottom load train
100	LTB20	Load Cell	9.95	LBS	1000	0.6% of Full Scale	strap 20, bottom load train
101	LTB21	Load Cell	9.95	LBS	1000	0.6% of Full Scale	strap 21, bottom load train
102	LTB22	Load Cell	9.95	LBS	1000	0.6% of Full Scale	strap 22, bottom load train
103	LTB23	Load Cell	9.95	LBS	1000	0.6% of Full Scale	strap 23, bottom load train
104	LTB24	Load Cell	9.95	LBS	1000	0.6% of Full Scale	strap 24, bottom load train
105	LTB25	Load Cell	9.95	LBS	1000	0.6% of Full Scale	strap 25, bottom load train
106	LTB26	Load Cell	9.95	LBS	1000	0.6% of Full Scale	strap 26, bottom load train
107	LTB27	Load Cell	9.95	LBS	1000	0.6% of Full Scale	strap 27, bottom load train
108	LTB28	Load Cell	9.95	LBS	1000	0.6% of Full Scale	strap 28, bottom load train
109	LTB29	Load Cell	9.95	LBS	1000	0.6% of Full Scale	strap 29, bottom load train
110	LTB30	Load Cell	9.95	LBS	1000	0.6% of Full Scale	strap 30, bottom load train
111	LTB31	Load Cell	9.95	LBS	1000	0.6% of Full Scale	strap 31, bottom load train
112	LTB32	Load Cell	9.95	LBS	1000	0.6% of Full Scale	strap 32, bottom load train
113	LRT01T	Linear	9.95	IN	6 ~ 12	0.013 IN	between straps 2 & 3, top load train
114	LRT02T	Linear	9.95	IN	6 ~ 12	0.013 IN	between straps 6 & 7, top load train
115	LRT03T	Linear	9.95	IN	6 ~ 12	0.013 IN	between straps 10 & 11, top load train
116	LRT04T	Linear	9.95	IN	6 ~ 12	0.013 IN	between straps 14 & 15, top load train
117	LRT05T	Linear	9.95	IN	6 ~ 12	0.013 IN	between straps 18 & 19, top load train
118	LRT06T	Linear	9.95	IN	6 ~ 12	0.013 IN	between straps 22 & 23, top load train
119	LRT07T	Linear	9.95	IN	6 ~ 12	0.013 IN	between straps 26 & 27, top load train
120	LRT08T	Linear	9.95	IN	6 ~ 12	0.013 IN	between straps 30 & 31, top load train
121	LRT01B	Linear	9.95	IN	6 ~ 12	0.013 IN	between straps 2 & 3, bottom load train
122	LRT02B	Linear	9.95	IN	6 ~ 12	0.013 IN	between straps 6 & 7, bottom load train
123	LRT03B	Linear	9.95	IN	6 ~ 12	0.013 IN	between straps 10 & 11, bottom load train
124	LRT04B	Linear	9.95	IN	6 ~ 12	0.013 IN	between straps 14 & 15, bottom load train
125	LRT05B	Linear	9.95	IN	6 ~ 12	0.013 IN	between straps 18 & 19, bottom load train
126	LRT06B	Linear	9.95	IN	6 ~ 12	0.013 IN	between straps 22 & 23, bottom load train
127	LRT07B	Linear	9.95	IN	6 ~ 12	0.013 IN	between straps 26 & 27, bottom load train
128	LRT08B	Linear	9.95	IN	6 ~ 12	0.013 IN	between straps 30 & 31, bottom load train
129	TC02	Type K	n/a	Deg_F	-300 ~ 2000	0.9 Deg F	Test Area Temp
130	P01_PSI	Pressure Transducer	9.95	PSI	0 ~ 30	0.25% of Full Scale	Test Article Pressure
131	SG01C	Calcultated Strain	n/a	MI_I	50,000	Developmental Instrumentation ~ 5% of Full Scale	at strap 9, upper cord
132	SG02C	Calcultated Strain	n/a	MI_I	50,000		at strap 9, lower cord
133	SG03C	Calcultated Strain	n/a	MI_I	50,000		between straps 8 & 9, upper cord
134	SG04C	Calcultated Strain	n/a	MI_I	50,000		between straps 8 & 9, lower cord
135	SG05C	Calcultated Strain	n/a	MI_I	50,000		at strap 29, upper cord
136	SG06C	Calcultated Strain	n/a	MI_I	50,000		at strap 29, lower cord
137	SG07C	Calcultated Strain	n/a	MI_I	50,000		between straps 28 & 29, upper cord
138	SG08C	Calcultated Strain	n/a	MI_I	50,000		between straps 28 & 29, lower cord
139	SG09C	Calcultated Strain	n/a	MI_I	50,000		at strap 21, upper cord
140	SG10C	Calcultated Strain	n/a	MI_I	50,000		at strap 21, lower cord
141	SG11C	Calcultated Strain	n/a	MI_I	50,000		between straps 20 & 21, upper cord
142	SG12C	Calcultated Strain	n/a	MI_I	50,000		between straps 20 & 21, lower cord
143	SG13C	Calcultated Strain	n/a	MI_I	50,000		between straps 13 & 14, upper cord mid point between straps
144	SG14C	Calcultated Strain	n/a	MI_I	50,000		between straps 13 & 14, lower cord closer to strap 14
145	SG15C	Calcultated Strain	n/a	MI_I	50,000		between straps 13 & 14, lower cord mid point between straps
146	SG16C	Calcultated Strain	n/a	MI_I	50,000		between straps 13 & 14, lower cord closer to strap 13